1.15 Advances in the Enzymology of Monoterpene Cyclization Reactions

Edward M. Davis, Washington State University, Pullman, WA, USA

1.15.1	**Introduction**	585
1.15.2	**Cyclization Chemistry**	588
1.15.2.1	Monoterpene Cyclases and Related Catalysts	588
1.15.2.2	Monoterpene Cyclase Enzymology	588
1.15.2.3	Ionization and Isomerization of Geranyl Diphosphate	590
1.15.2.4	Cyclization Reaction Stereochemistry	591
1.15.2.5	Formation of Monoterpene Structural Types	593
1.15.2.6	Molecular Biology of the Monoterpene Cyclases	594
1.15.3	**Structural Studies**	595
1.15.3.1	Structural Commonalities	595
1.15.3.2	(−)-(4*S*)-Limonene Synthase	598
1.15.3.3	(+)-Bornyl Diphosphate Synthase	600
1.15.3.4	1,8-Cineole Synthase	603
1.15.4	**Conclusions**	605
References		606

1.15.1 Introduction

Monoterpenes are widely occurring, likely ubiquitous natural products found in the plant kingdom and are the primary contributors to the organoleptic properties associated with various herbs, spices, citrus, conifers, and most flowers and fruits. These 10-carbon, short-chain terpenes, often in combination with sesquiterpenes (C15) and diterpenes (C20), exhibit many ecological roles, including broad-spectrum antimicrobial, allelopathic, herbivore deterrent (indirect and direct), and pollinator attractant properties.[1–4] The diversity of monoterpenes generated from the cyclization of the predominant monoterpene precursor, geranyl diphosphate (GPP (**28**)), or its *cis*-isomer, neryl dliphosphate (NPP), results in several general monoterpene types (**Scheme 1**), with greater multiplicity achieved by the cyclase through stereochemical and regiochemical alterations. Downstream enzymatic transformations of these initial manifolds through hydroxylations, dehydrogenations, double-bond and/or carbonyl reductions, isomerizations, and conjugations can lead to increased biodiversity as exemplified in the mint family (**Scheme 2**).[5–7] The primary subject of this review is the enzyme-mediated generation of the initial monoterpene scaffolds by monoterpene cyclases (or synthases).

Comprehensive and historical reviews of monoterpene biosynthesis were published in 1987[8] and in this series in 1999;[9] the present contribution will provide an overview of the mechanistic and structural advances that have been made since that time including recent enzyme inhibitor studies, structural studies, and cyclase mutagenesis in the context of a more comprehensive monoterpene cyclization model. While highlighting the recent advances made in the past decade, I would be remiss if I did not acknowledge and build upon the seminal findings made by the terpene giants of the past and present, from Kekulé, Wallach, and Rüzicka to Croteau, Coates, and Cane.

Because many aspects of monoterpene chemistry were revealed by previous work, and thoroughly reviewed in a variety of contexts,[8–12] a judicious appraisal of these principles will supplement the latest findings in the framework of our current state of understanding. This review is divided into two main sections. The first section is an overview of monoterpene cyclization chemistry including the general properties of cyclases and isomerization, cyclization, and carbocation rearrangements that precede reaction termination. A brief consideration of the molecular biology of monoterpene cyclases will provide a segue to the second section, which will consider the mechanistic specificity of three monoterpene cyclases that catalyze ostensibly different reaction types, and provide the structural basis for each enzyme.

(1) Myrcene
(2) *Z*-β-ocimene
(3) *E*-β-ocimene
(4) Linalool
(5) Geraniol
(6) Limonene
(7) Terpinolene
(8) β-phellandrene
(9) α-terpinene
(10) α-terpineol
(11) 1,8-cineole
(12) α-pinene
(13) β-pinene
(14) Pinan-2-ol
(15) α-thujene
(16) Sabinene
(17) Sabinene hydrate
(18) Bornyl diphosphate
(19) Borneol
(20) 3-carene
(21) 2-carene
(22) Camphene
(23) Camphene hydrate
(24) Fenchol
(25) Tricyclene

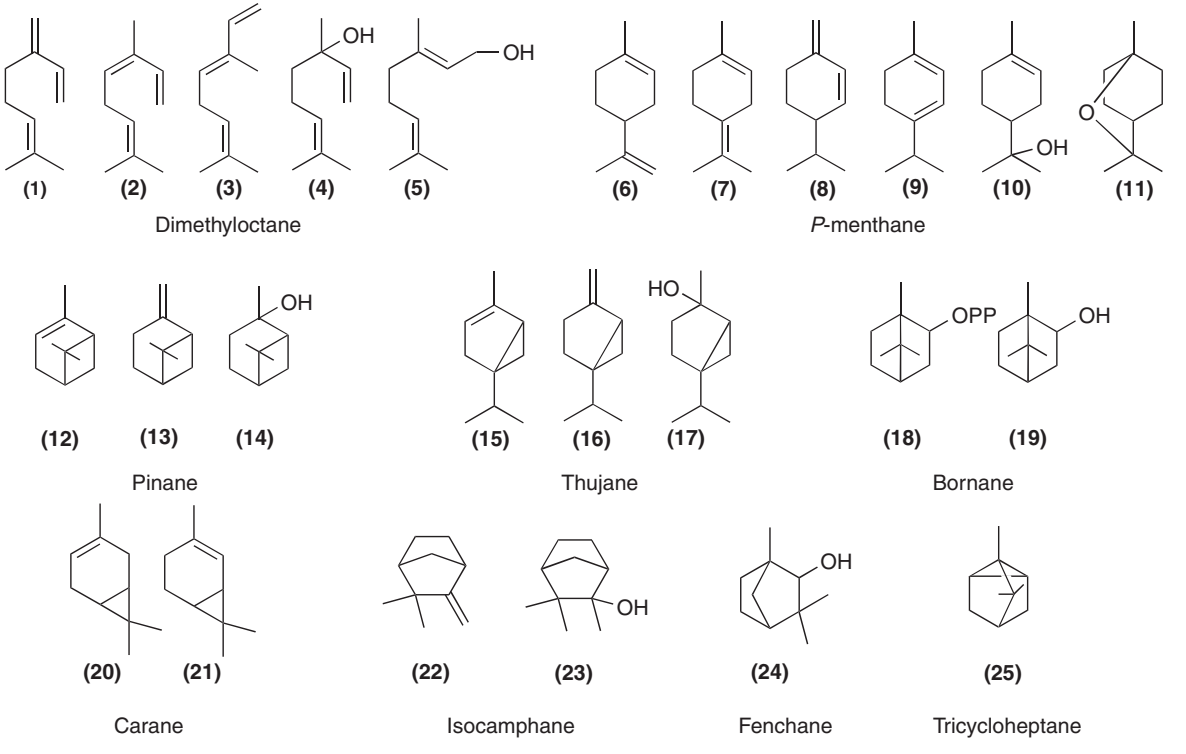

Scheme 1

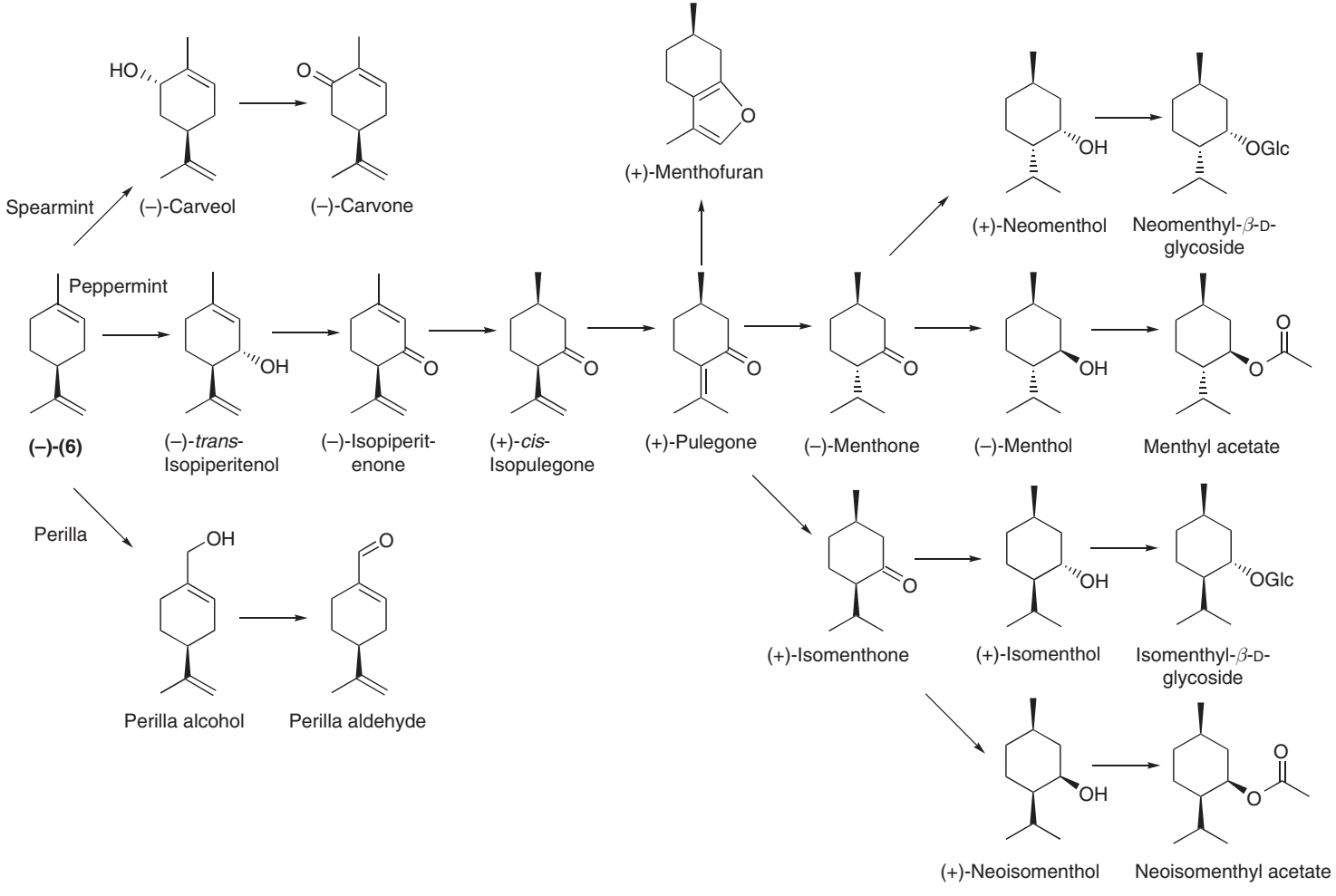
HO
O
Spearmint
(–)-Carveol
(–)-Carvone
(+)-Menthofuran
OH
OGlc
(+)-Neomenthol
Neomenthyl-β-D-glycoside
Peppermint
OH
O
O
O
O
OH
O
O
(–)-(6)
(–)-trans-Isopiperitenol
(–)-Isopiperit-enone
(+)-cis-Isopulegone
(+)-Pulegone
(–)-Menthone
(–)-Menthol
Menthyl acetate
Perilla
OH
O
OH
OGlc
(+)-Isomenthone
(+)-Isomenthol
Isomenthyl-β-D-glycoside
Perilla alcohol
Perilla aldehyde
OH
O
(+)-Neoisomenthol
Neoisomenthyl acetate

Scheme 2

1.15.2 Cyclization Chemistry

1.15.2.1 Monoterpene Cyclases and Related Catalysts

Terpene cyclases catalyze intramolecular, electrophilic C–C bond formation of allylic prenyl diphosphate substrates (GPP (**28**), NPP, farnesyl diphosphate (FPP (**29**)), and geranylgeranyl diphosphate (GGPP)) in a reaction analogous to the intermolecular condensations of the prenyltransferase family of bisubstrate enzymes (isoprenyl diphosphate synthases) in which an allylic Δ^2 prenyl diphosphate (**27**) and a Δ^3 prenyl diphosphate (**26**) are combined in a 1′-4 linkage (**Scheme 3**).[13,14] This linkage is prototypical in the chain elongation prenyltransferases including GPP synthase, but other condensation reactions that result in cyclopropyl (1′-2-3), branched (1′-2), or cyclobutyl (1′-2-3-2′) diphosphates have undergone recent characterization using prenyltransferase chimeras;[15] yet little is known regarding the downstream enzymology of the biosynthesis of the so-called irregular monoterpenes (**Scheme 4**). The cyclases and *trans*-prenyltransferases are structurally (discussed in Section 1.15.3.1) and mechanistically similar,[16,17] and it is notable that examples of prenyltransferases that catalyze cyclization-type reactions[18–20] and a cyclase that catalyzes a coupled prenyltransferase–cyclase reaction[21] have been reported (**Scheme 5**). Common to both enzyme types is the generation of highly reactive carbocation intermediates by diphosphate ionization (or in some diterpene cyclases double-bond protonation) with subsequent carbon–carbon bond formation resulting from electrophilic addition to a π-system, and reaction termination.[8,17] In contrast to the straightforward prenyltransferase reaction, terpene cyclase catalysis often involves myriad rearrangements and further cyclizations facilitated by guided carbocation movements throughout the initial and subsequently formed ring systems before termination by multiple nucleophile capture strategies, leading to an amazing structural diversity of terpenes.[8–10]

1.15.2.2 Monoterpene Cyclase Enzymology

The monoterpene cyclases are quite similar to the sesquiterpene and diterpene cyclases in physicochemical properties[8–10,22] and have adopted largely similar strategies for substrate binding and product formation.[16,22]

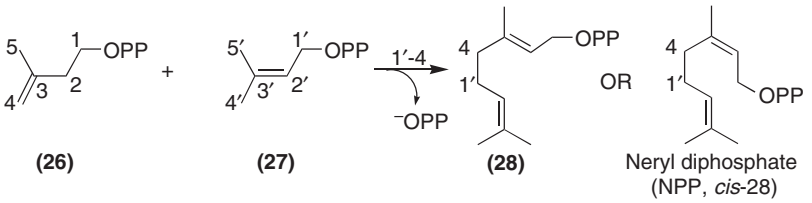

Scheme 3

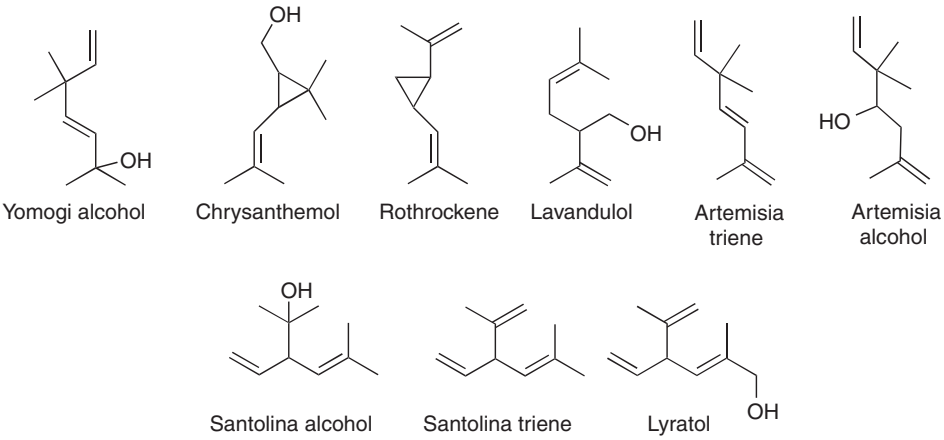

Scheme 4

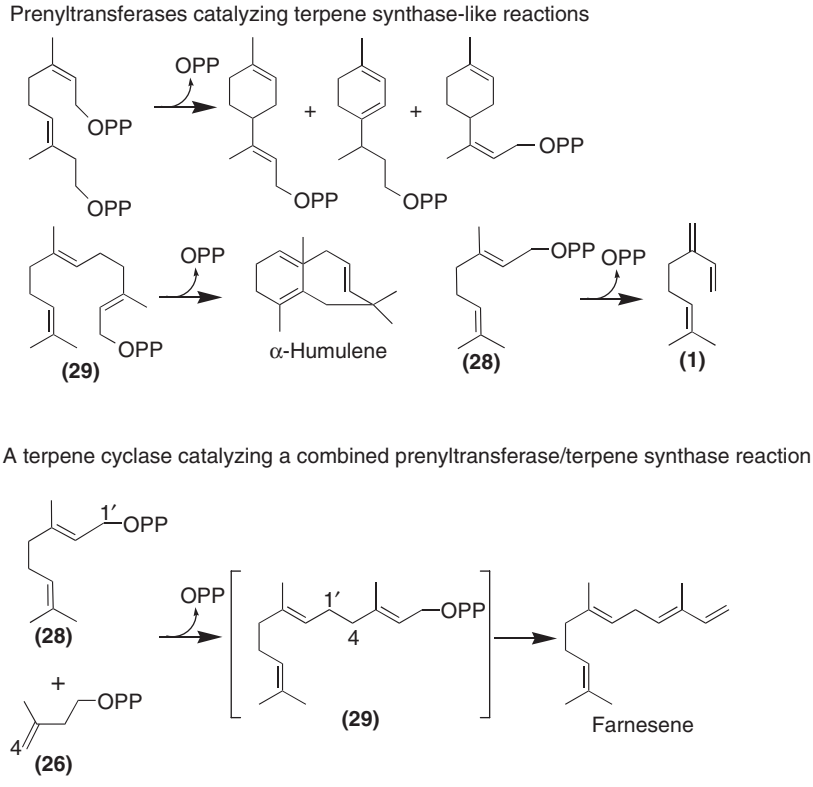

Scheme 5

The very nature of the cyclization reactions of these three cyclase types and the common electrophilic carbocation attack on remote π-bonds suggest that the greater flexibility of the longer prenyl chains (C10 vs. C15 and C20) and the additional double bonds in their respective substrates will increase potential product diversity. Although essentially true, it is equally clear that the cyclization chemistry of the monoterpene cyclases is no less complex than that of their sesquiterpene and diterpene cyclase counterparts and, in that context, the monoterpene cyclases provide an adequate and simplified model for terpene cyclase chemistry.

Regarding the general properties of plant monoterpene cyclases, they are functionally soluble, 50–70 kDa monomers or homodimers, require a divalent cation (usually Mg^{2+} or Mn^{2+}), sometimes monovalent cation (K^+), have K_m values in the low micromolar range, and have relatively low turnover numbers ($<1\ s^{-1}$).[8–10,17] Most monoterpene cyclases are multiproduct enzymes with promiscuity profiles (level of minor products) ranging from trace to greater than 60% of the total, with product diversity often including several monoterpene structural types (**Scheme 1**) generally of essentially one enantiomeric series but near racemic cyclase products are known.[23–24] Yet, despite the apparent active site flexibility needed to generate such product diversity, monoterpene cyclases are generally specific in using only C10 prenyl diphosphate substrates, GPP (**28**), linalyl diphosphate (LPP (**30**)), or NPP (*cis*-isomer of **28**).[8–10]

GPP is generally considered the natural C10 substrate of monoterpene cyclases[8–10] and early cell-free attempts to define substrate preference utilized a variety of cyclases representative of diverse plant families and nearly all monoterpene skeletal types and, despite the mechanistically facile, direct cyclization of the *cis*-Δ^2 prenyl diphosphate (NPP), most monoterpene cyclases preferred the *trans*-Δ^2 prenyl diphosphate (GPP)[25–29]. These studies were confounded by the preferential enzymatic hydrolysis of GPP (over NPP and LPP) by the contaminating phosphatases in the crude preparations; a situation remedied by further purification and separation of the competing activities and resulting in near universal preference for GPP.[30] However, recent characterization of the two recombinant enzymes, a prenyl transferase and a monoterpene cyclase, from cultivated tomato have clearly identified that the prenyl transferase is an NPP (**30**) synthase (presumably by

typical 1′-4 elongation, **Scheme 3**) and that the cyclase (β-phellandrene synthase) catalytic efficiency for NPP is 10^{14}-fold higher than for GPP.[31] As this is the first authenticated NPP synthase and the first, dedicated NPP cyclase the significance of this finding is considerable in the context of substrate availability and preference, and has mechanistic implications for substrate binding and ionization. It is notable that cyclization of NPP is an isomerization-independent reaction yet this cyclase retains the ability to catalyze the normally, tightly coupled isomerization–cyclization of GPP to β-phellandrene (**8**), albeit at reduced rates; an observation that may have evolutionary implications. This finding is consistent with the discovery in wild tomato of a *cis*-FPP synthase and a corresponding *cis*-sesquiterpene cyclase,[32] a cyclase also capable of cyclization of NPP but not GPP to α-terpineol (**10**). Regarding substrate preference, it is notable that ample studies have identified authentic GPP synthases from multiple, diverse plant families,[33–39] and as such, the taxonomic extent and significance of this finding await further biochemical characterization of enzymes from diverse plant families. It should also be noted that the universality of the α-terpinyl carbocation and the subsequent series of internal additions, cyclizations, rearrangements, and reaction terminations leading to the characteristic mono-, bi-, and tricyclic monoterpenes and monoterpenols (and diphosphate esters) catalyzed by both the *cis*- and *trans*-cyclases is in accord with the mechanistic model presented herein and reviewed elsewhere.[8–10]

Methodical characterization of monoterpene cyclases from their native plant sources has afforded details on the mechanistic aspects of the cyclization cascade for enzymes that catalyze products of each structural type and stereochemistry and, as a body of work, has provided a detailed and comprehensive model of monoterpene cyclization.[8–10] Building on these initial cyclase studies, characterization of monoterpene cyclases from liverworts, ferns, and algae[40–42] has demonstrated that these 'lower eukaryote' cyclases resemble their higher plant counterparts in basic enzymological characteristics and suggests a common plant monoterpene cyclase progenitor. In contrast, recent cloning and characterization of the first microbial monoterpene cyclase[43,44] bolsters earlier evidence (from sesquiterpene cyclases) that microbial cyclases evolved catalytic function independently from plant cyclases yet have adopted similar strategies for binding the prenyl diphosphate substrate and catalyzing the electrophilic reaction.[16,22]

1.15.2.3 Ionization and Isomerization of Geranyl Diphosphate

The predominant precursor to monoterpene cyclization, GPP (**28**), is geometrically precluded from direct cyclization due to the *trans* geometry of the C2–C3 double bond, and hence requires ionization and isomerization to the linalyl system to accommodate C1–C2 bond rotation (**Scheme 6**, carbon numbering is based on **28**).[8] In support of the intermediacy of the tertiary intermediate, cyclization of LPP (**30**) by the monoterpene cyclases is ubiquitous, and product profiles thus generated are usually similar to those obtained with **28**; catalytic efficiency favors the cyclization of **30** over **28** by at least twofold,[45–49] whereas geraniol (**5**), linalool (**4**), and nerol (and their monophosphate esters) are not catalytically competent.[25,50,51] Successful demonstration of the electrophilic nature (and thus ionization) of the cyclization reaction was achieved through studies

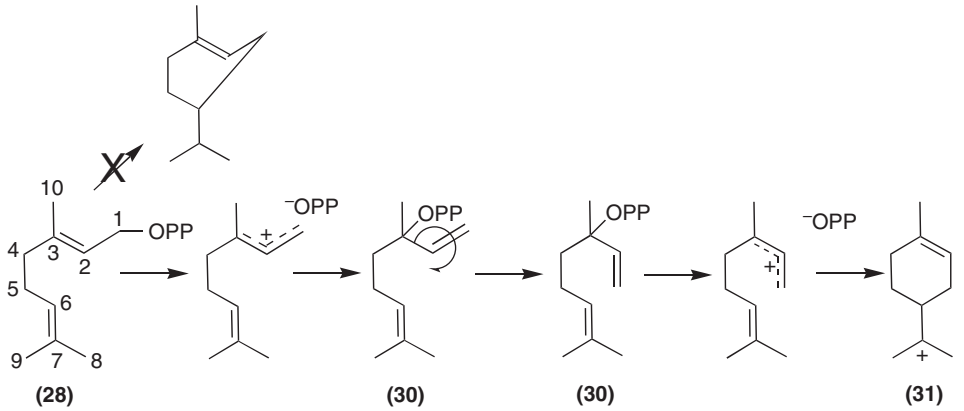

Scheme 6

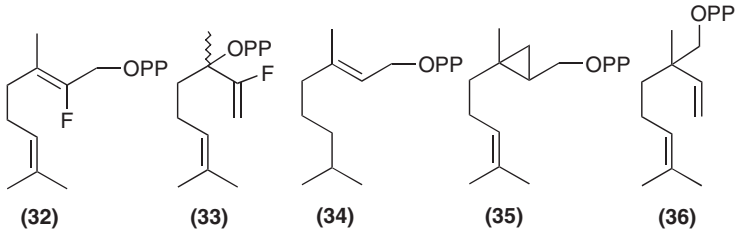

Scheme 7

using the fluorinated, electron-withdrawing analogs 2-F-GPP (**32**) and 2-F-LPP (**33**) (**Scheme 7**) with the monoterpene cyclases[52,53] that showed minimally 100-fold rate suppressions and further provided evidence that the cyclase reaction is initiated by separate ionizations of **28** and **30**. The electrophilic nature of the reactions of sesquiterpene cyclases and *trans*-prenyltransferases was also demonstrated using appropriate allylic, fluorinated substrate analogs.[54,55] Recent kinetic analyses using these monoterpene analogs with purified, recombinant (−)-limonene synthase ((−)-LS) and (+)-bornyl diphosphate synthase ((+)-BS) have bolstered this early work with native cyclases and demonstrated that both fluoroanalogs are effective competitive inhibitors with inhibition constants in the low micromolar range (6–79 $\mu mol\,l^{-1}$).[56] Furthermore, the competitive nature of the inhibition is evidence that both ionizations occur in the same active site.

The intermediacy of LPP (**30**) in the reaction cycle had never been directly observed and, coupled with the greater cyclization efficiency of **30** versus **28** by the cyclases, suggests a tightly coupled reaction sequence.[8,9] The noncyclizable analogs 6,7-dihyroGPP (**34**) and 2,3-cyclopropyl GPP (**35**) (**Scheme 7**) were used with native cyclases in an effort to directly observe the release of the corresponding LPP analogs and, in all cases tested, products were identified that were entirely consistent with the formation of **30** including preliminary identification of 3-homoLPP (**36**), the expected LPP analog derived from the isomerization of 2,3-cyclopropyl GPP (**35**).[57,58] This work was repeated with purified, recombinant (−)-LS, (+)-BS, and (−)-pinene synthase ((−)-PS) in an attempt to generate products at increased quantities for unambiguous identification and stereochemical assignment.[59] Unfortunately, no detectable diphosphorylated monoterpenes were generated, though product type and stereochemistry did permit identification of several mechanistic distinctions between these different cyclase types, most notably in the biosynthesis of significant quantities of monoterpenols from both analogs with (+)-BS but not from the olefin cyclases (−)-PS and (−)-LS. Structural evidence for these apparent differences will be discussed in Section 1.15.3.3.

Although the studies with the substrate analogs (described above) failed to detect the formation and release of the cryptic tertiary intermediate, and despite the low turnover demonstrated by (−)-LS of 2-F-GPP (**32**) and 2-F-LPP (**33**) to fluorolimonene,[56] these analogs were successfully used in the crystallization of (−)-LS (see Section 1.15.3.2).[60] Fortuitously, (−)-LS crystallized in the presence of **32** catalyzed the isomerization of **32** to **33**, wherein the electron-withdrawing properties of the allylic fluorogroup prevented the second ionization and subsequent cyclization. This represents the first direct demonstration of LPP as an intermediate in monoterpene cyclization observed in the context of the active site, and presumably in a conformation relevant to cyclization.

1.15.2.4 Cyclization Reaction Stereochemistry

During the course of ionization and isomerization of GPP (**28**), the first chiral center is established at C3 of LPP (**30**), and its significance in the stereochemistry of subsequent transformations and in product formation is absolute. The ability to successfully separate this two-component reaction pathway using exogenous substrates of enantiomeric purity has provided the opportunity to elucidate several mechanistic and stereochemical aspects of monoterpene cyclization (these experiments were reviewed by Croteau,[8] Wise and Croteau,[9] and Davis and Croteau[10]), and has led to the development of a comprehensive model of monoterpene cyclization.[8] The model suggests that the stereochemical outcome is likely a consequence of initial binding of **28** in the cyclase active site in either a right-handed or a left-handed helical orientation and, following ionization, there occurs suprafacial migration of the diphosphate across the C1–C2–C3 plane to produce (3*S*)-LPP or (3*R*)-LPP, exclusively (**Scheme 8(a)**). A transoid to cisoid transition of the enantiomers of **30** is dependent on C1–C2 bond

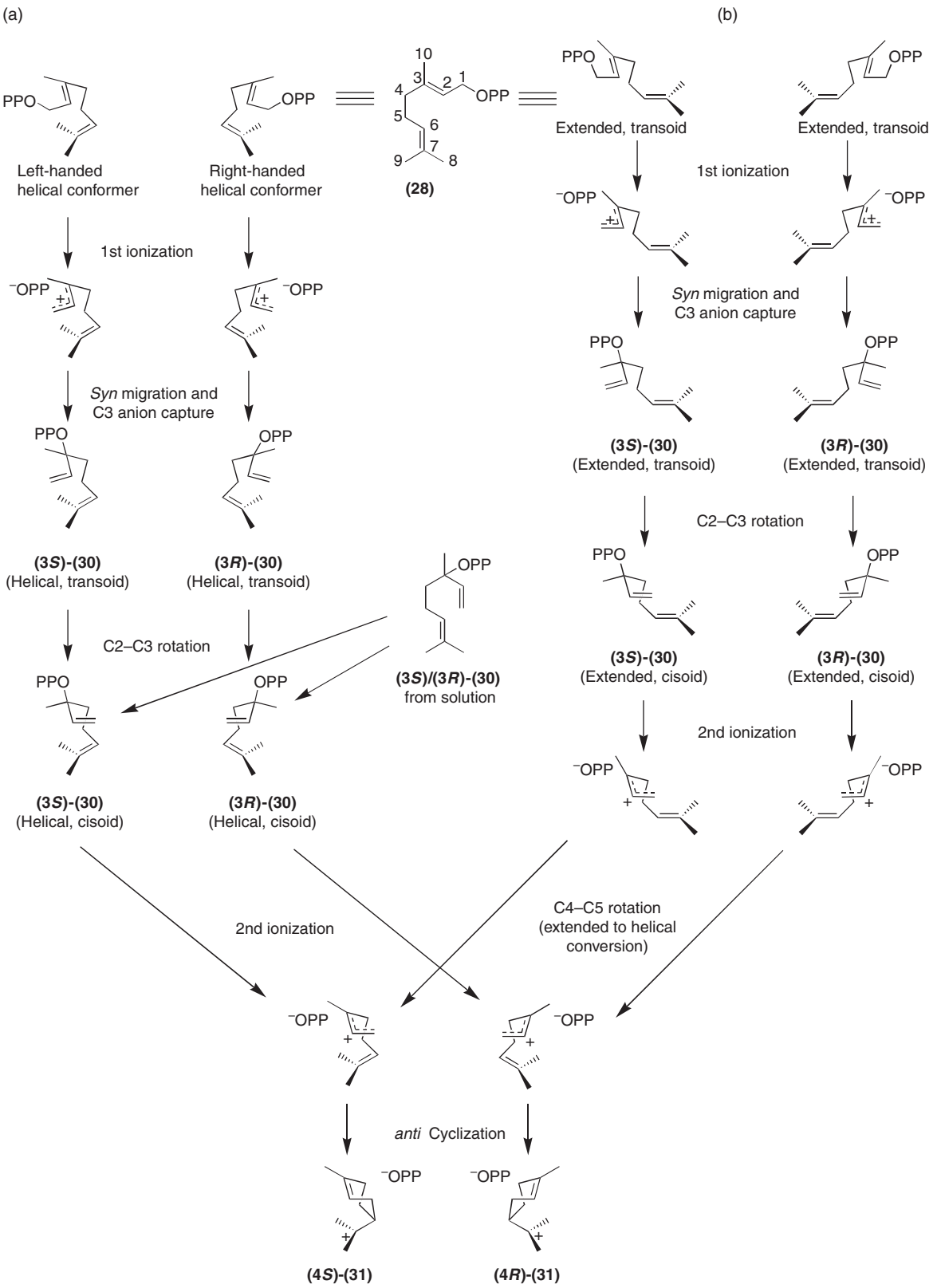
(a)
(b)
PPO
OPP
10
3
2
1
4
5
6
7
9
8
(28)
Left-handed helical conformer
Right-handed helical conformer
Extended, transoid
1st ionization
⁻OPP
Syn migration and C3 anion capture
(3S)-(30) (Helical, transoid)
(3R)-(30) (Helical, transoid)
(3S)-(30) (Extended, transoid)
(3R)-(30) (Extended, transoid)
C2–C3 rotation
(3S)-(30) (Extended, cisoid)
(3R)-(30) (Extended, cisoid)
2nd ionization
(3S)-(30) (Helical, cisoid)
(3R)-(30) (Helical, cisoid)
(3S)/(3R)-(30) from solution
C4–C5 rotation (extended to helical conversion)
anti Cyclization
(4S)-(31)
(4R)-(31)

Scheme 8

rotation, precedes ionization of **30**, and is necessary for proper juxtaposition of C1 with C6 to facilitate π-cation cyclization. Following the ionization of **30**, cyclization occurs *anti*, *endo* (*anti* refers to the face of C1 bond formation relative to the face of C1 diphosphate departure and *endo* refers to the spatial orientation of the olefinic chain) to produce the (4*S*)-α-terpinyl cation from (3*S*)-(**30**) and the (4*R*)-α-terpinyl cation from (3*R*)-(**30**) with subsequent formation of products of the (−)- and (+)-antipodal series, respectively. The consequence of *syn*-migration of the diphosphate and *anti*, *endo* cyclization is that the overall retention of configuration at C1 will be observed in the product. Retention of configuration has been clearly established for numerous cyclases in separate assays using (1*R*)- and (1*S*)-[^{3}H]-GPP; following cyclization of the respective substrate, the product was converted to a ketone wherein a stereoselective, base-mediated proton exchange permitted stereochemical determination and deduction of configuration at C1 of the substrate.[46,47,61–63] These results, coupled with the stereospecificity of cyclization of either (3*R*)- or (3*S*)-(**30**), fully support the model outlined.[62,63]

As noted in the previous section, enzymatically formed 2-F-LPP (**33**) was observed in the (−)-LS crystal structure, and it is noteworthy that electron density was consistent with **33** in an extended, transoid orientation, which suggests that GPP (**28**) binds similarly.[60] Thus, a refinement of the cyclization model was presented (**Scheme 8(b)**) in which **28** binds and isomerizes to **30** in the extended, transoid conformer, an orientation from which the electrophile is too distant from the π-system for cyclization to occur, and after C2–C3 bond rotation attains the extended, cisoid conformation. Finally, ionization of **30** and C4–C5 bond rotation presents the helical, cisoid linyl cation for cyclization. It is notable that 2-F-LPP (**33**), when crystallized with (−)-LS, is bound in the helical, cisoid conformer (an orientation competent for cyclization), and thus likely represents an artifact of presentation to the cyclase in an energetically favored form (from solution) rather than as an intermediate in the dynamic reaction cascade but, nonetheless, suggests that the C4–C5 bond rotation occurs after the second ionization, or the rotation is sufficiently slow such that no interchange occurs in the crystalline state.[60]

Having established stereochemical considerations for GPP isomerization to specific stereoisomers of LPP, and their cyclization to (4*R*)- and (4*S*)-α-terpinyl cation by a common monoterpene cyclase mechanism, it is clear that further manipulations are enzyme specific and, thus, the central importance of the α-terpinyl carbocation (**31**) in product formation cannot be overemphasized. This universal cyclohexenoid carbocation, as a consequence of its formation from either (*R*)- or (*S*)-LPP, determines the stereochemical outcome of the products, and its precise orientation in, and its interactions with, the cyclase active site determines if and how the course of carbocation migration through hydride shifts, secondary electrophilic cyclizations, and C–C bond rearrangements will proceed prior to reaction termination.

1.15.2.5 Formation of Monoterpene Structural Types

The acyclic dimethyloctane monoterpenes result from premature deprotonation of, or water capture of, the geranyl or linalyl cations, and afford *cis*-/*trans*-ocimene (**2**)/(**3**) or myrcene (**1**), or linalool (**4**) and geraniol (**5**). The simplest set of cyclic monoterpenes are the *p*-menthane type, which result from alternate, direct deprotonations of the α-terpinyl carbocation (**31**) (**Scheme 9**) to generate limonene (**6**) or terpinolene (**7**) or, involve water capture to generate α-terpineol (**10**) (which following protonation of the C–C double bond (of α-terpineol) and internal addition leads to 1,8-cineole (**11**)). A 1,2- or a 1,3-hydride shift (delocalization of charge on the latter secondary allylic cation leads to the more stable tertiary cation) and subsequent deprotonations produce α- and γ-terpinene (**9** and **38**, respectively) and α- and β-phellandrene (**37** and **8**, respectively). The thujane monoterpenes proceed by a 1,2-hydride shift followed by cyclopropyl ring closure and tertiary cation quench, by deprotonation in the case of α-thujene (**15**) and sabinene (**16**), or by water capture to produce sabinene hydrate (**17**). Carane monoterpenes undergo opposing 1,3-proton eliminations from C3 or C5 to generate the cyclopropyl ring of 2-carene (**21**) and 3-carene (**20**), respectively. The pinane and bornane monoterpenes undergo bicyclization at opposing ends of the remaining double bond of the α-terpinyl cation (**31**) to generate the favored tertiary cation (pinyl cation (**39**)) or a less-favored, anti-Markovnikov secondary cation (bornyl cation (**40**)). Alternate deprotonations of the former generate α-pinene (**12**) and β-pinene (**13**), whereas diphosphate or water capture leads to bornyl diphosphate (BPP (**18**)) and borneol (**19**), respectively. Wagner–Meerwein (W–M) rearrangements of the bornyl cation (**40**) (6,2-rearrangement) and pinyl cation (**39**) (3,1-rearrangement) lead to

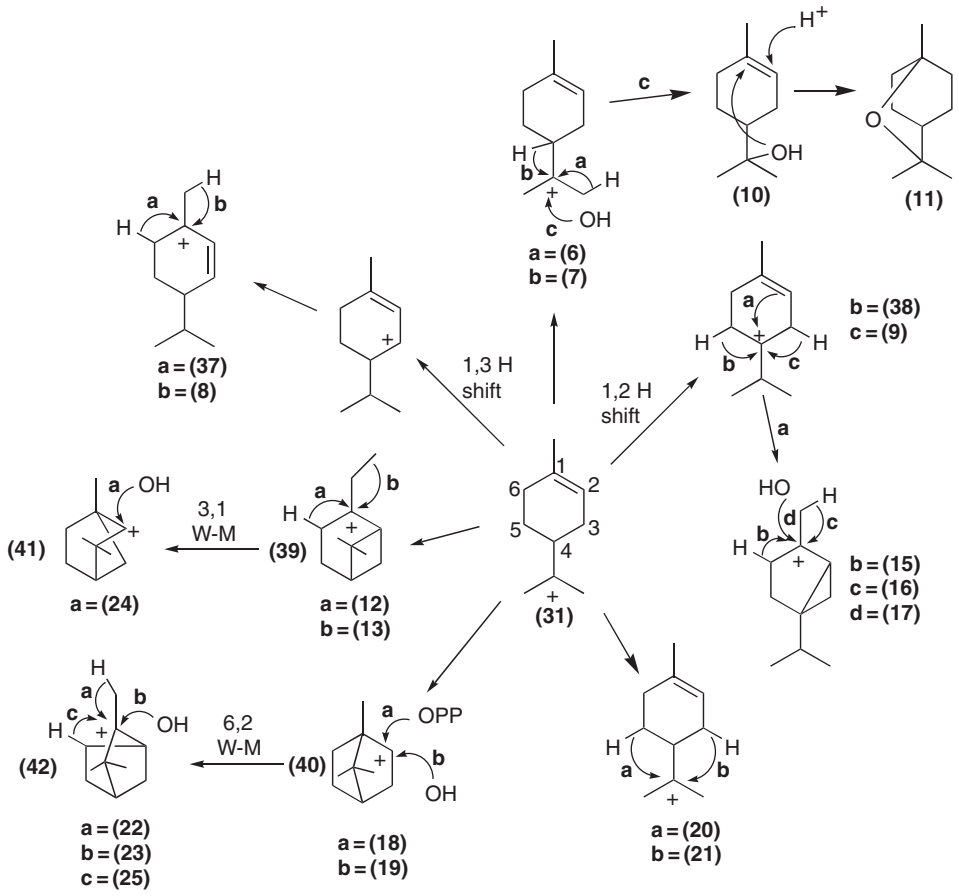

Scheme 9

the isocamphyl (**42**) and fenchyl (**41**) cations, respectively. In the latter case, water capture leads to fenchol (**24**), whereas termination in the former case by deprotonation, water capture, or a deprotonation-mediated ring closure results in camphene (**22**), camphene hydrate (**23**), and tricyclene (**25**), respectively.

It is significant that the above descriptions, meant to provide a survey of cyclic monoterpene chemistry, should in no way be considered complete. Each carbocation may undergo alternate electrophile capture (i.e., water capture rather than deprotonation), and capture may occur from different faces of the carbocation, situations that expand the cyclase repertoire and clearly emphasize potential cyclase versatility.

1.15.2.6 Molecular Biology of the Monoterpene Cyclases

Although it is clear that a limited number of monoterpenes are generated as a result of monoterpene cyclases (estimated at 30–40[8,9]), the promiscuous nature of these cyclases suggests an infinite number of permutations in product distributions, reflected by changes in amino acid sequence and thereby structure.

Consistent with this observation, recent genome projects suggest that terpene synthase (TPS) genes are present in very high numbers: *Arabidopsis*, not previously recognized as a prolific terpene-producing plant, has at least 40 TPS genes;[64] black cottonwood, *Populus trichocarpa*, has nearly 50;[65] and a wine grape sequencing project has identified 89 TPS genes (of these, the authors estimate that 35 are monoterpene cyclases).[66] Currently, at least 50 recombinant monoterpene cyclases from multiple, evolutionarily conserved and diverse plant sources have been characterized, and as a group they generate most of the major monoterpene structural types, each with a different degree of reaction promiscuity (based on the types and ratios of minor products) that provides a vast resource for structural and mechanistic studies previously not possible.

An alignment of representative monoterpene cyclases indicates that enzymes from quite diverse plant sources nonetheless retain high conservation, and several highly conserved sequence motifs are apparent (**Figure 1**). The TPSs are classified according to sequence relatedness and thus phylogenetic origin, and fall into seven subfamilies, TPS-a through TPS-g.[67–69] Angiosperm monoterpene synthases fall largely into the TPS-b and TPS-g subfamilies, whereas their gymnosperm counterparts are members of TPS-d, a complex family with further subdivisions.[69] The subfamilies b and d are not exclusive to monoterpene cyclases nor are they completely inclusive of all C10 cyclases, an observation that suggests that the evolution of terpene cyclases has proceeded along multiple paths; subfamilies g and f contain mostly acyclic monoterpene synthases.[69] A complementary classification system considers the inton–exon structure and intron number of these cyclase genes, and a proposal for evolutionary descent from a presumed progenitor cyclase was developed based on intron gains and losses through evolutionary time.[70,71] A recent *in silico* survey of *Arabidopsis* TPS genes uncovered evidence for multiple gene duplication events and significant clustering of cyclases and prenyltransferases, and suggests a mechanism for the observed diversity of terpene cyclases and their respective products and pathways.[68] Genome analysis and cyclase gene categorization systems are instructive and, in the context of the immense sequence data available, provide a means for gene characterization. However, it must be stressed that terpene cyclase activity is not predictable from sequence; characterization, coupled with enzymological and structural studies, is far more informative.

1.15.3 Structural Studies

1.15.3.1 Structural Commonalities

As noted earlier, the mechanistic resemblance between the prenyltransferases and terpene cyclases is striking, though little sequence homology is shared. Not surprisingly, there is considerable sequence homology among the plant terpene cyclases, and common evolutionary lineages have been noted;[16,67,68] however, the microbial cyclases, which catalyze similar reaction types and generate structurally related products, share no sequence similarity with their plant counterparts (nor among themselves),[9,10,22] and neither group shares significant sequence similarity with the prenyltransferases.[72] In spite of these primary structural differences, a common α-helical fold has been adopted by these enzyme types to accommodate similar chemistries.[16,22,60,73–75] This active site fold has been termed the 'class I TPS fold' and contrasts with the structurally unrelated, α-helical 'class II TPS fold' common to the C30 triterpene cyclases.[16,72] The latter catalysts initiate carbocation formation by C–C double bond or epoxide protonation instead of initiation by diphosphate ester ionization, but cyclization chemistry proceeds through electrophilic addition to π-systems similar to the short-chain terpene cyclases. Notably, the plant diterpene cyclase, abietadiene synthase, catalyzes a protonation-initiated cyclization and an ionization-initiated cyclization in two separate active sites,[76] and although no structure has been solved for this bifunctional cyclase, homology suggests that it will adopt a fold characteristic of the known plant terpene cyclases.[10,16]

Structures are available for four plant terpene cyclases: the sesquiterpene cyclase, 5-*epi*-aristolochene synthase,[77] and three monoterpene cyclases (discussed below).[60,73,78] The structural similarities between these cyclases are consistent with their largely shared mechanistic and physicochemical properties and permit several generalizations to be made (**Figure 2**). The typical plant TPS is a bidomain structure with N- and C-terminal domains of approximately 8 and 12 α-helices, respectively. Structures obtained using a variety of substrate, intermediate, and product analogs suggest that the N-terminal domain has no direct role in catalysis and has adopted a gluconase/glucoamylase-like fold with similarity to the class II fold of triterpene cyclases.[16,72] No known function has been attributed to this domain but its absence from the microbial cyclases, and the experimental evidence that catalytic specificity of plant monoterpene and sesquiterpene cyclases resides in the C-terminal domain,[79–81] suggests that it may be relictual; yet its considerable sequence conservation suggests otherwise. A notable element of the N-terminal domain consists of a largely unstructured loop at the terminus that becomes ordered upon substrate binding and caps the active site cavity, presumably to prevent solvent access to the highly reactive carbocations. A potential role for residues of this loop in monoterpene cyclase catalysis is discussed below.

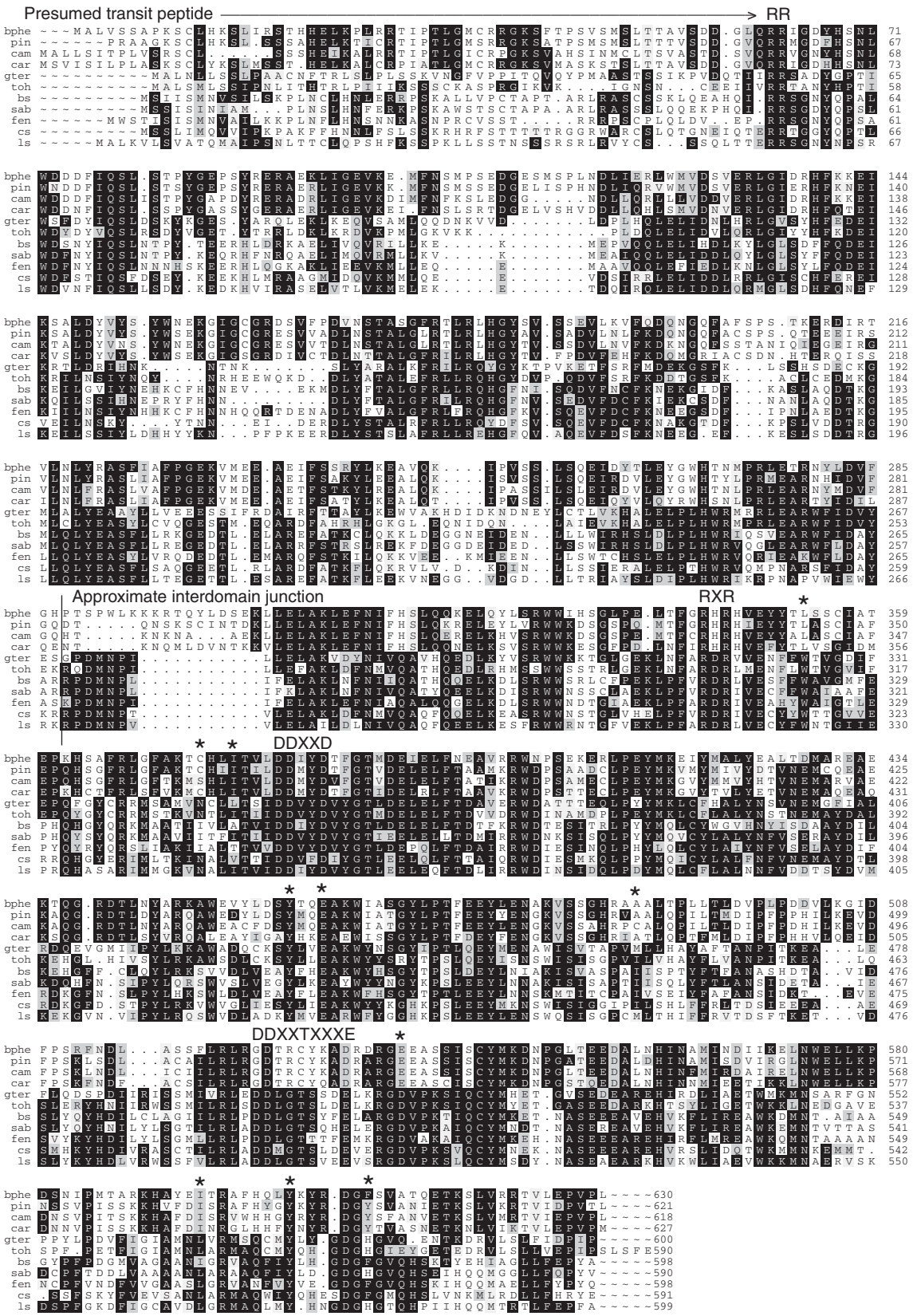
Presumed transit peptide
RR
Approximate interdomain junction
RXR
DDXXD
DDXXTXXXE

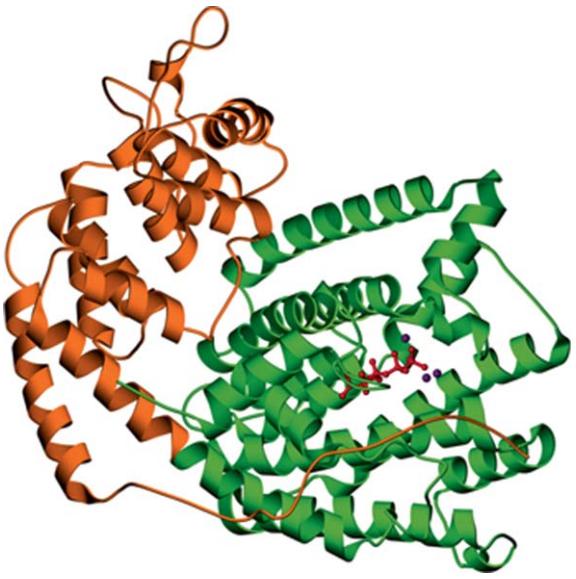

Figure 2 Ribbon plot of a monomer chain of (−)-LS showing the helical N-terminal domain (orange) and C-terminal active site domain (green). The analog 2-F-LPP (red) and the divalent cation Mn^{2+} (purple) are shown and were used in cocrystallization. Note the orientation of the N-terminal loop over the active site opening. Reproduced with permission from D. C. Hyatt; B. Youn; Y. Zhao; B. Santhamma; R. M. Coates; R. B. Croteau; C.Kang, *Proc. Natl. Acad. Sci. U.S.A.* **2007**, *104*(13), 5360–5365. Copyright 2007 National Acadamy of Sciences, USA.[60]

Analog-bound structures provide additional evidence that cyclization chemistry occurs exclusively within the C-terminal domain, in a cavity commonly composed of a handful of α-helices and adjoining loops. Typical active site features have been noted, including a polar, active site opening for diphosphate binding and a relatively deep, hydrophobic prenyl-binding pocket replete with aromatic residues.[16,60,73,77,78] The strategy for allylic diphosphate binding is shared among the plant terpene cyclases, and has many notable similarities with FPP synthase[10,16] and the microbial cyclases,[16,22,82] including a conserved DDxx(D/E) motif involved in diphosphate coordination through divalent cations. In addition to this highly conserved aspartate-rich motif, plant cyclases have an adjacent (in space) RxR motif and an opposing (D/N)Dxx(T/S)xxxE motif (designated the DTE/NSE motif), which provide all the requisite features for diphosphate recognition and ionization by the typical plant cyclases (**Figure 1**).[16] A conspicuous lack of DTE/NSE motif conservation is apparent in the gymnosperm monoterpene cyclases and suggests that these enzymes have adopted an alternate diphosphate-binding feature. Gymnosperm cyclases also exhibit monovalent cation dependence (K^+) and a conserved serine, several residues downstream from the modeled location of the angiosperm NSE/DTE motif, was implicated in K^+-binding by site-directed mutagenesis of a spruce (−)-PS (corresponding to residue S541 in bphe, **Figure 1**).[92] The precise nature of the divalent and monovalent cation interactions with the alkyl diphosphate in the gymnosperm monoterpene cyclase active sites awaits the determination of a representative structure.

Figure 1 Alignment of representative monoterpene cyclase amino acid sequences. The plastid-targeting sequence is shown with an approximate cleavage site indicated. Conserved sequence motifs are noted above their respective locations. The positions of selected active site residues of (+)-BS, (−)-LS, and CS are identified with an asterisk. The key to abbreviations (with accession numbers and plant sources): bphe, β-phellandrene synthase (AF139205), *Abies grandis*;[83] pin, (−)-α/(−)-β-pinene synthase (AAS47692), *Picea abies*;[84] cam, (−)-camphene synthase (AAB70707), A. grandis;[85] car, (+)-3-carene synthase (AAO73863), *P. abies*;[86] gter, γ-terpinene synthase (AAM53943), *Citrus limon*;[87] toh, α-terpineol synthase (AAS79352), *Vitis vinefera*;[88] bs, (+)-bornyl diphosphate synthase (AAC26017), *Salvia officinalis*;[89] sab, (+)-sabinene synthase (AAC26018), *S. officinalis*;[89] fen, fenchol synthase (AAV63790), *Ocimum basilicum*;[90] cs, 1,8-cineole synthase (ABH07677), *Salvia fruticosa*;[78] ls, (−)-limonene synthase (AAC37366), *Mentha spicata*.[91]

The three mechanistically unique monoterpene cyclase structures are presented in the context of the mechanistic and stereochemical analyses of their respective reaction cascades (from the α-terpinyl cation (**31**) to product) to provide substantive details. Therefore, it is important to consider each active site cavity as promoting ostensibly different reaction cascades, and in that context to seek out structural differences. The first enzyme presented, (−)-LS, catalyzes a simple deprotonation to (−)-limonene (**6**) and generates only minor amounts of side products, all of which are olefinic and of the (−)-antipodal series. In contrast, (+)-BS terminates its reaction three-quarters of the time by diphosphate capture, produces largely (+)-series monoterpenes, and is relatively promiscuous in terminating its remaining reaction cycles by deprotonation. The final structure considered is that of 1,8-cineole synthase (CS), a cyclase that has a stable monoterpenol intermediate (that debinds occasionally), requires π-bond protonation before cyclic ether formation, and terminates one-third of its reaction cycles by deprotonation.

1.15.3.2 (−)-(4*S*)-Limonene Synthase

Limonene (**6**) is a common component of many plant essential oils, and biotransformation of the (−)-antipode in the mints leads to a variety of scented compounds (**Scheme 2**), whereas in *Citrus* the (+)-antipode is largely responsible for the characteristic 'peel aroma' associated with oranges. Investigations using (−)-LS as a model monoterpene cyclase have provided a wealth of information regarding mechanistic (reviewed by Croteau,[8] Wise and Croteau,[9] and Davis and Croteau[10]) and, recently, structural aspects of this, the simplest of all monoterpene cyclizations.[60] Considerable enzymological evidence obtained with (−)-LS has provided support for the general model of isomerization and cyclization of GPP to the (4*S*)-α-terpinyl cation (as outlined in the previous section) and supports the general application of this model.[8–10]

Several informative studies were undertaken with antipodal LSs, and with two sage PSs that generate either (+)- or (−)-limonene (**6**) in significant side reactions. One study sought to determine the nature of methyl deprotonation of the α-terpinyl cation (**31**) by (+)- and (−)-LS and the PSs and used [8-^{3}H]-GPP with chemical derivitization-assisted product analysis to determine that methyl deprotonation occurs exclusively from the *cis*-methyl (C9) for the antipodal cyclases from *Citrus* and *Mentha*[93–95] (an observation consistent with natural abundance NMR[96]), whereas the PSs showed little discrimination between *cis*- and *trans*-methyl deprotonation. These results suggest that dedicated LSs (of either enantiomer) may be more restrictive in α-terpinyl cation (**31**) binding than a cyclase that is more committed to other reaction types (i.e., bicyclization by PS). Stereochemical determination of the methyl-to-methylene elimination was accomplished with assays of the mint (−)-LS using C9-trilabeled GPP (^{1}H, ^{2}H, and ^{3}H). The NMR-based analysis demonstrated *anti*-elimination (relative to C1–C6 bond formation) and suggests a precisely positioned isopropyl group with clearly defined contacts that are maintained through the cyclization cascade.[95] The above experimental evidence provides a comprehensive stereochemical model for the deprotonation of the (4*S*)-(**31**) to yield limonene (**6**) (**Scheme 10**).

Intramolecular isotope effects associated with the methyl-methylene elimination (in limonene (**6**) production) were determined using the mint (−)-LS and the PSs and [8,8,9,9-$^2H_4$]-GPP.[95] Significant effects were demonstrated for all three cyclases as expected, and are consistent with primary kinetic isotope effects associated with deuterium elimination. These experiments provided a means (using [8,9-$^2H_6$]-GPP) to observe isotopically sensitive branching effects with these multiproduct cyclases, since the branch point between **6** and pinene production requires C8- or C9-deprotonation or bicyclization, respectively.[95] Quite unexpectedly, no significant isotope effect was observed for all three cyclases, and it was suggested that the lack of competition between monocyclization and bicyclization is due to the presence of conformational isomers of the α-terpinyl cation (**31**),

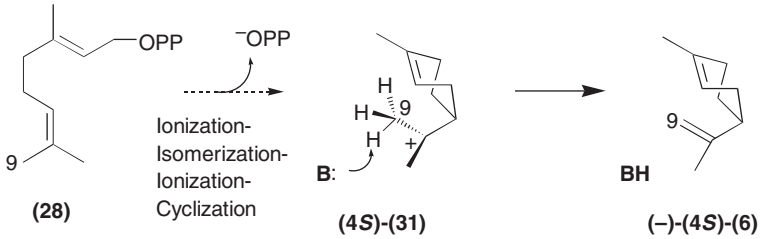

Scheme 10

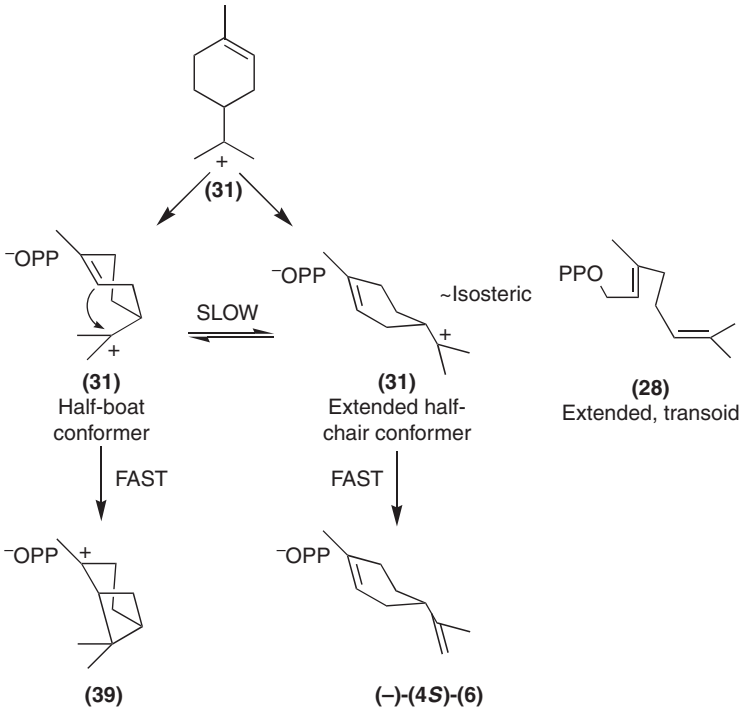

Scheme 11

the extended half-chair and the half-boat, respectively, whose interchange in the active site is slow compared with deprotonation or bicyclization (**Scheme 11**).[95] The prescience of this proposal made in the absence of cyclase structural information is notable in the light of the recent crystallographic studies of (−)-LS, in which 2-F-GPP (**32**) was isomerized to 2-F-LPP (**33**) and adopted an extended, transoid orientation that is nearly isosteric to the extended, half-chair orientation of the predicted α-terpinyl conformer that leads to limonene (**6**) (**Scheme 11**). It is tempting to speculate that the extended, transoid conformation of **33**, observed in the active site of (−)-LS, is reflective of an active site contour that promotes the extended half-chair conformer of the **31** for generation of **6**; the half-boat conformer required for pinene production occurs rarely in a dedicated LS.

(−)-LS was cloned and characterized from *Mentha spicata*[91] and has typical terpene cyclase properties,[97,98] including reaction kinetics and a preference for Mg^{2+}. This enzyme is minimally promiscuous in generating largely **6** and essentially only products of the (−)-antipodal series (**Scheme 12**). The latter observation is

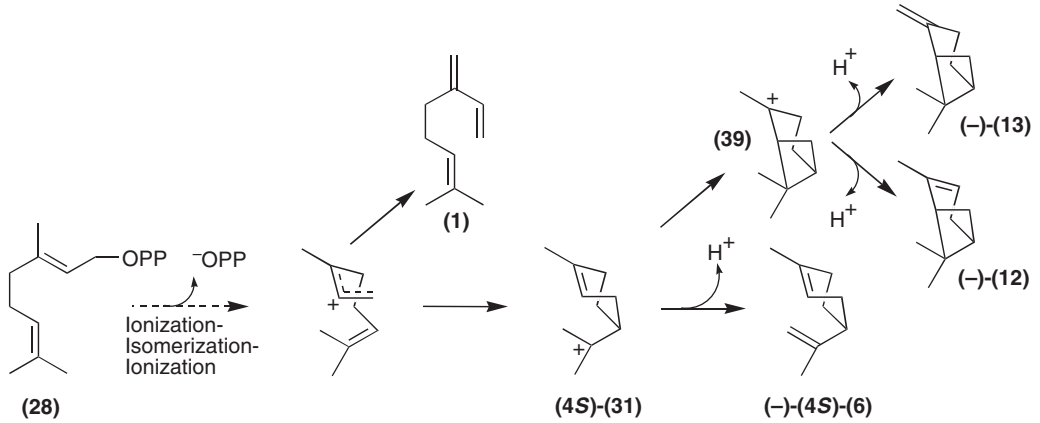

Scheme 12

entirely consistent with the mechanistic studies presented that suggest a very restrictive active site cavity. Native (−)-LS has been localized to the plastid[99] and its modest expression from the full-length cDNA construct suggested that removal of the N-terminal targeting peptide for expression and characterization might be fruitful. A series of N-terminal truncations (using the cDNA) and kinetic analyses of the resultant recombinant proteins identified a pseudomature form of (−)-LS that included the highly conserved, tandem arginine motif (**Figure 1**, (−)-LS residues 58 and 59) and provided a cyclase with kinetics comparable to native (−)-LS.[100] Mutagenesis or removal of either arginine resulted in isomerization-incompetent cyclases whose cyclization capacity was intact (modest cyclization of LPP was demonstrated with truncation to residue 89), suggesting that the tandem arginine motif is involved in the binding or recognition of GPP, or in the isomerization of GPP to LPP, but not in cyclization chemistry, *per se*.

As noted earlier, the structure of (−)-LS from *M. spicata* was obtained using the substrate and intermediate analogs 2-F-GPP (**32**) and 2-F-LPP (**33**), respectively, and **32** was isomerized in the (−)-LS crystal to **33**, which adopted an extended, transoid orientation.[60] On the contrary, **33**, presented from solution, bound in the helical, cisoid conformer (**Schemes 8(a) and 8(b)**).[60] The (−)-LS structure is typical of plant cyclases (**Figure 2**, described above) and assumes a homodimer in the crystalline state, in contrast to studies on the native enzyme that suggest monomer formation in solution.[98] Binding of the substrate and intermediate analogs and three divalent metal ions occurs exclusively in the C-terminal domain; no direct interaction between substrate or intermediate analogs occurs in the N-terminal domain. The active site is in closed conformation with the terminal, tandem arginine residues providing bonding interactions with the C-terminal residues, E363, Y435, and the backbone carbonyl of V357. It is probable that active site closure occurs upon diphosphate binding, and that initiation of the isomerization step cannot happen without this interaction. Three Mn^{2+} ions (Mn^{2+} was used for crystallization rather than the preferred cation Mg^{2+}) and the diphosphate are clearly positioned in the active site lip but subunit differences exist and suggest that alternate diphosphate binding orientations arise even in the highly restrictive (−)-LS active site. The prenyl-binding cavity of (−)-LS is largely hydrophobic with two prominent aromatic residues, Y573 and W324, positioned below the isopropyl group. These are perhaps involved in π-carbocation stabilization of the α-terpinyl cation (**31**), a stabilization of mechanistic significance given the regio- and stereospecificity of the terminating methyl-methylene elimination. Potential termination nucleophiles are plentiful (i.e., backbone carbonyls, active site waters, and the diphosphate anion), and, given the reactivity of the carbocations, any of several proximal residues could also fulfill this role (B: in **Scheme 10**); a suitably positioned asparagine (N345) and histidine (H579) are attractive candidates. An active site histidine was predicted by substrate-mediated protection in the presence of a histidine-directed reagent.[101] Clearly, the (−)-LS structure provides critical information on the structural determinants of a simple monoterpene cyclase for which there exists extensive mechanistic information, but perhaps of greater significance are the mechanistic implications uncovered by the use of fluoroanalogs with this enzyme, which provides details of substrate binding and conformation in the context of the isomerization component of the monoterpene cyclase reaction cycle. It is not clear at this time whether the binding conformation of the enzyme-generated 2-F-LPP (**33**) is specific to (−)-LS or is a more universal aspect of monoterpene cyclization.

1.15.3.3 (+)-Bornyl Diphosphate Synthase

The (+)- and (−)-antipodes of camphor are especially fragrant components in the oils of sage and tansy, respectively, and the committed step in their biosynthesis is catalyzed by the antipodal BSs from the respective plants. An immense body of work has contributed to the understanding of many aspects of the reactions of these cyclases and to the more general monoterpene cyclase mechanism discussed above and previously reviewed in detail.[8,9] It is instructive, however, to discuss several aspects of the cyclization cascade that are specific to (+)-BS and contribute to the context of the (+)-BS crystal structure.

Displacement of the diphosphate from C1 to C3 (isomerization) and from C3 to C2 (termination) suggests that (+)-BS must have unique structural features compared to other cyclase types to accommodate this apparent movement of the diphosphate anion. A series of positional isotope effect studies were conducted that used [1-^{18}O]-GPP, [α-^{32}P]-GPP, [β-^{32}P]-GPP, and the correspondingly labeled LPP compounds to determine the extent of diphosphate scrambling in the course of the reaction to BPP (**18**).[102,103] Product

analysis involved derivitization and MS analysis for the [^{18}O]-BPP and selective monophosphate hydrolysis and radio analysis for the [^{32}P]-BPP. The cumulative results of these studies unambiguously demonstrated that the phosphoester oxygens of substrate and product are unchanged, suggesting an ordered removal and movement of the diphosphate without P–O–P bond rotation or end-to-end exchange.

A comparison of inhibitory properties between (+)-BS and (−)-LS using 2-F-GPP (**32**) and 2-F-LPP (**33**) found that these competitive inhibitors had largely similar K_i values for both cyclases except in the case of **32** with (+)-BS (10-fold lower inhibition constant).[56] This contrast in inhibition may be reflective of differences in active site architecture that are specific to the different reaction chemistries of these cyclases. Such differences are also supported by inhibitor studies conducted with (+)-BS, (−)-LS, and a gymnosperm (−)-PS using the analogs 6,7-dihydroGPP (**34**) and 2,3-cyclopropylGPP (**35**).[59] The strictly olefin cyclases, (−)-LS and (−)-PS, generated largely hydrocarbon products from these analogs, whereas (+)-BS generated mostly monoterpenols, suggesting access and involvement of water in the (+)-BS reaction, which is not observed in the normal reaction cycle. The involvement of this normally unreactive water in the (+)-BS reaction will be addressed below, in the context of the structure.

Bicyclization in the BS reaction cascade may proceed through two different pathways, direct cyclization to the bornyl cation (**40**) (anti-Markovnikov) and cyclization to the pinyl cation (**39**) followed by rearrangement to **40**. Evidence gained from isotopically sensitive branching experiments (using [10-$^2H_3$]-GPP) with two sage PSs (both cyclases generate camphene (**22**) and α-pinene (**12**)) demonstrated that bicyclization to **40** (en route to **22**) proceeded directly (anti-Markovnikov cyclization) in one case and through the transient **39** with subsequent rearrangement to **40** in the other case.[104,105] Thus, precedent was established for both mechanisms of bicyclization by these olefin cyclases. The bicyclization mechanism for (+)-BS is not known but it has been suggested that the localization of the diphosphate over C2 could polarize the C1–C2 double bond, thus leading directly to **40** formation, as a consequence of diphosphate positional effects.[106]

Studies using [8-^{2}H]-GPP and [9-^{2}H]-GPP, coupled with NMR analysis of products, were able to localize the position of the *trans*-methyl of GPP as the *syn* geminal methyl of BPP, thus demonstrating that bicyclization occurs on the same face of the C6–C7 bond of GPP on which primary C1–C6 cyclization had occurred.[106] The studies outlined above have established considerable details regarding different aspects of the (+)-BS reaction cascade and provide a stereochemical model of bicyclization and anion capture (**Scheme 13**).

(+)-BS was cloned and characterized from *Salvia officinalis* and it is quite similar to (−)-LS in physicochemical properties.[89] Based on the studies described above for (−)-LS, (+)-BS localization to the plastid is presumed. Poor expression of the soluble preprotein, and the presence of N-terminal tandem arginines, led to the production of a 'mature' recombinant cyclase truncated immediately upstream of this motif. This pseudomature form resembles the native enzyme in all properties evaluated including product profile (**Scheme 14**).[89]

(+)-BS was the first monoterpene cyclase for which structures were determined.[73] Judicious selection of analogs that mimic all intermediates and the product of the reaction (**Scheme 15**) has provided structures for which binding interactions during the isomerization–cyclization cascade can be inferred.[73] In general, results obtained were consistent with the plant cyclase structures described above. The structure of the native (+)-BS (without analog) had considerable disorder in the N-terminal loop and two active site regions, one that includes part of the DTE motif (active site lip) and the other that is deep within the prenyl-binding cavity (F578-S583). Analog or product binding promotes significant conformational changes that result in ordering through two significant interdomain interactions (involving hydrogen bonds between the penultimate R (of the tandem R-motif) and a downstream Y (of the N-terminal loop) with the first and third D of the DDxxD motif,

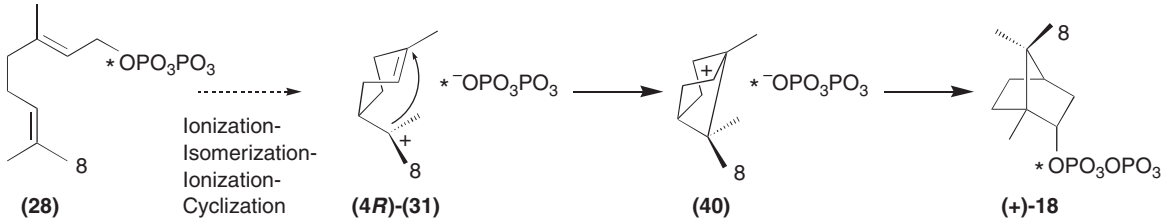

Scheme 13

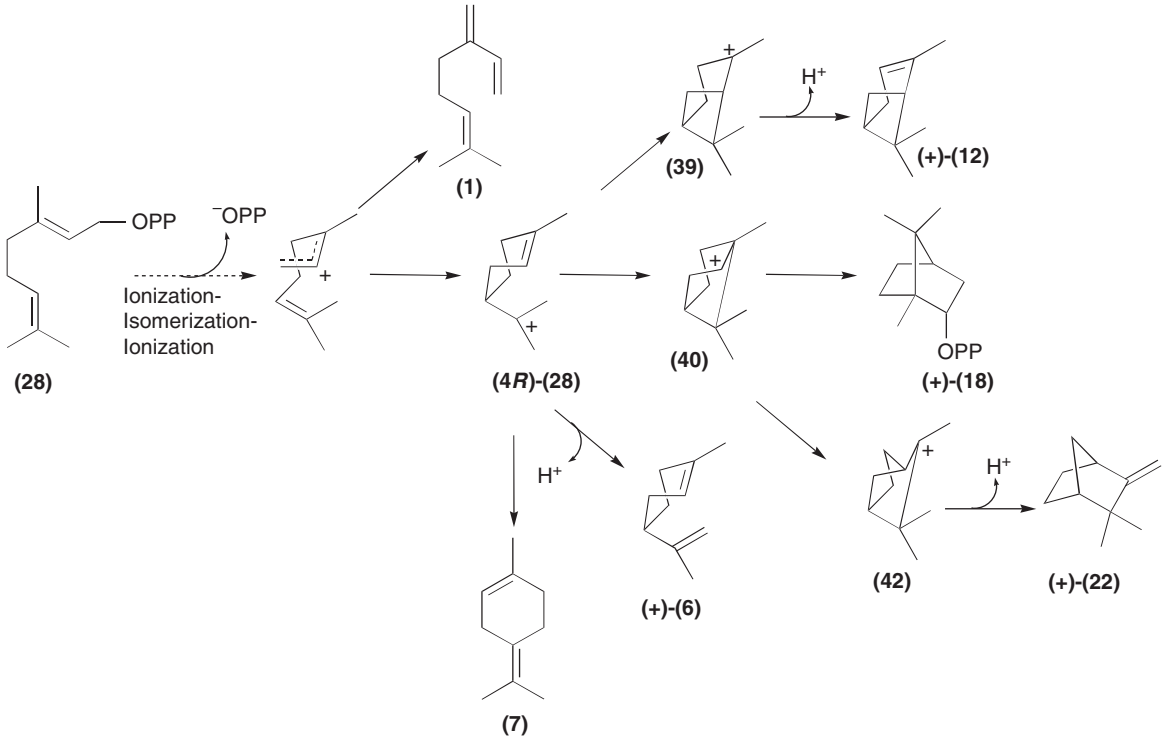

Scheme 14

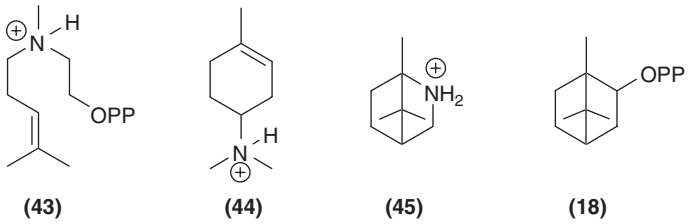

Scheme 15

respectively) that cap the active site cavity. The first and third D residues also participate in Mg^{2+} coordination and coordinate a tightly held water; the second D (of the DDxxD motif) is salt-linked to R314 of the RxR motif. The conspicuous presence of a water molecule near the active site lip is consistent with monoterpenol production by (+)-BS observed during turnover of the noncyclizable analogs 2,3-cyclopropylGPP (**34**) and 6,7-dihydroGPP (**35**), as discussed earlier (**Scheme 7**). In the normal reaction cascade of (+)-BS, no monoterpenols are formed and this suggests that the tightly held water performs a structural or catalytic role.[73] The orientation of the diphosphate in all of the structures is largely unchanged, and this group is held in position by Mg^{2+} coordination and three hydrogen bonds (residues R493, R314, and K512), thereby suggesting that the requisite and precise repositioning of the diphosphate observed during the reaction cycle (C1–C3–C2 migration) is facilitated by corresponding movements of the prenyl carbocations. This suggestion is supported by the structure with the 2-aza-bornane analog (**45**, bornyl cation mimic), which is positioned with the charged aza group within 3 Å of the oxygen that would become the phosphoester oxygen of product (described above). Interestingly, the 7-aza-7,8-dihydrolimonene analog (**44**) (an α-terpinyl cation mimic) bound upside down, likely an indication that cation interactions with the diphosphate counterion are important. The unproductive binding of this analog emphasizes the difficulties that may be encountered when intermediates are presented from solution rather than generated at the active site during which numerous protein conformational changes

may occur. This phenomenon is reminiscent of (−)-LS binding exogenous 2-F-LPP (**33**) in a helical, cisoid conformer versus the extended, transoid orientation adopted by **33** produced at the active site by isomerization of 2-F-GPP (**32**). A similar phenomenon was observed with the sage PSs, which generated altered product mixtures when presented with either LPP enantiomer from solution (compared to GPP-generated product profiles).[107]

The prenyl group of the analogs participates in van der Waals forces with three hydrophobic residues in the active site pocket, W323, I344, and F578. Such aromatic residues are similarly positioned in (−)-LS, and likely contribute, in both cases, to α-terpinyl carbocation (**31**) stabilization through π-cation interactions. Although termination by anion capture is regio- and stereochemically very precise, (+)-BS is moderately promiscuous during 25% of its reaction cycles in producing olefin co-products. Thus, orchestrated 'tumbling and folding' of the olefinic chain within the active site must occur to allow rearrangements before deprotonation from at least six different carbons (**Scheme 14**).

1.15.3.4 1,8-Cineole Synthase

1,8-Cineole (**11**, eucalyptol) is an achiral aromatic component of many plants, including *Salvia* and *Eucalyptus* leaves, has recently been identified as a rhizosphere volatile in *Arabidopsis*,[108] is well known as an allelopathic agent from *Salvia* and *Artemisia*,[109,110] and has folivore deterrent activity.[111] The generation of **11** by the namesake cyclase is atypical in that a second, stable (and chiral) intermediate (α-terpineol (**10**)) is formed at the active site and requires protonation of the endocyclic double bond to proceed to end product. Stereochemical studies with the 1,8-CS from *S. officinalis* demonstrated a kinetic preference of (*R*)-LPP over (*S*)-LPP, thus supporting the intermediacy of the (4*R*)-α-terpinyl cation and (4*R*)-(**10**).[112] Confirmation of (4*R*) stereochemistry was achieved by enzymatic cyclization of [1-^{3}H]-GPP with chemical conversion of the resultant (1*R*)-[3-^{3}H]-1,8-cineole to the corresponding butanediol ketal for stereochemical assignment.[112]

The origin of the ether oxygen was evaluated using [1-^{18}O]-GPP, [3-^{18}O]-LPP, and $H_2^{18}O$ in three separate experiments, and significant enrichment in the bridge oxygen occurred only with water as the nucleophile.[112] Recombinant enzyme (provided from an *S. officinalis* clone[89]) provided the means to generate sufficient product for NMR analysis, and the *syn* stereochemical disposition of water capture by the α-terpinyl cation (**31**) (addition on the inside face) was thus verified using [1,1,8,8,8-$^{2}H_5$]-GPP and [1,1,9,9,9-$^{2}H_5$]-GPP as substrates.[113] Enzymatic cyclization in the presence of D_2O and NMR analysis of the product confirmed *syn* addition at C6 (of the endocyclic double bond) and, thus, suprafacial ether bridge formation.[113] This work has firmly established the nature of cyclization of GPP to the achiral product by CS from *S. officinalis* (**Scheme 16**).

CS was cloned and characterized from *Salvia fruticosa*, and a pseudomature form of this cyclase (presumed transit peptide removed) was utilized for crystallization.[78] A single structure was obtained that displayed typical TPS features as described for (+)-BS and (−)-LS, and displayed only minor backbone differences with these cyclases in the active site region. The enzyme had a disordered N-terminal loop and two disordered C-terminal regions, similar to the (+)-BS native structure, which is likely a consequence of assuming the 'unbound conformation'. It should be noted that the structural studies (described below) and the mechanistic studies (described above) are from two closely related CSs that share 95% amino acid identity and have similar reaction profiles (**Scheme 17**). However, relatedness and high homology do not imply similar stereochemistry,

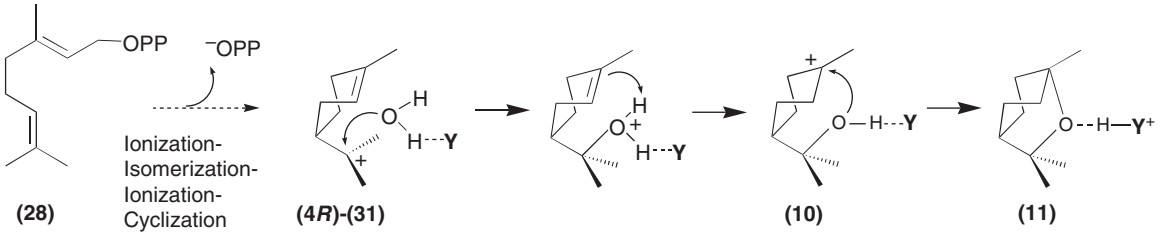

Scheme 16

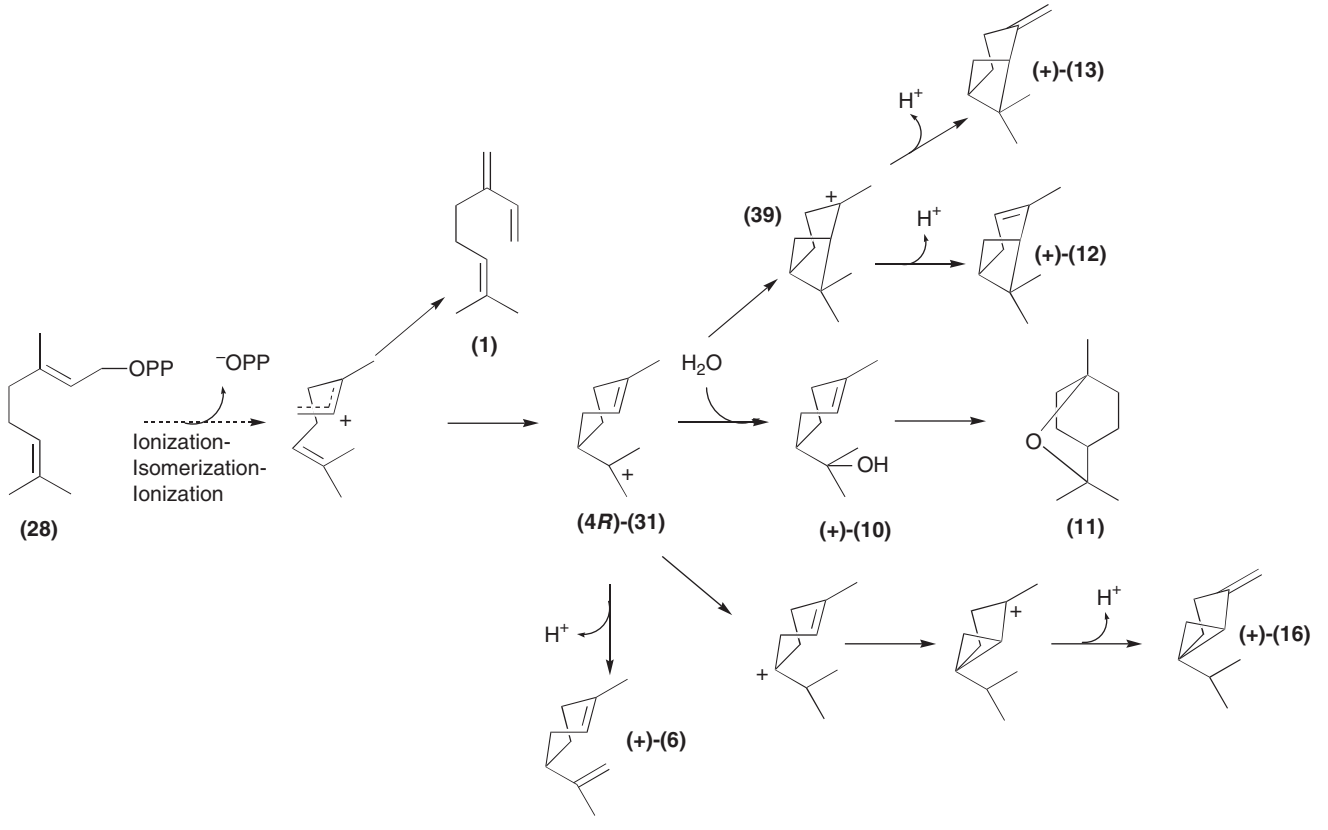
OPP
$^{-}$OPP
Ionization-
Isomerization-
Ionization
(28)
(1)
(4R)-(31)
H_2O
(39)
(+)-(13)
(+)-(12)
(+)-(10)
(11)
(+)-(6)
(+)-(16)
H^+

Scheme 17

a situation encountered with two enantiomeric maize sesquiterpene cyclases.[114] Nonetheless, the mechanistic studies provide ample detail for this enzyme type and provide enhanced context of this structural study.

Sequence alignments of the related *Salvia* cyclases (two sabinene synthases (SSs), two CSs, and (+)-BS) coupled with careful examination of the active site cavity identified an active site asparagine, located near the bottom of the hydrophobic cavity, that affects product outcome.[78] This residue, N338, coordinates an active site water in the CS structure (**Scheme 16**, Y = N338) that is notably absent in the (+)-BS (different location from the water discussed above in the (+)-BS structure) and (−)-LS structures. The N338I mutant (CS scaffold and SS residue) successfully eliminated all cation capture by water and increased sabinene (**16**) production by 15-fold relative to wild-type CS activity (with minimal kinetic effects); the reciprocal change in SS had little effect on product generation. Additional mutagenesis of the neighboring residue (and residues on the opposing face of the active site cavity) provided mild synergistic effects on the CS-to-SS conversion but had little effect on the reverse conversion. Further substitutions at N338 (L, V, A, C, and S) had pronounced effects on product ratios of the CS, with only small changes in catalytic efficiency.[78] Sesquiterpene synthase activity (normally not present in wild-type CS) was observed in three of the mutants (A, C, and S), consistent with the smaller overall side-chain size of the substitutions (relative to N), the presumed absence of water, and with the position near the bottom of the prenyl-binding cavity. The C15 products were largely analogous in structure to the C10 products generated by these mutants, and this suggests that the reaction cascades were similar, irrespective of chain length, such that the 'extra' five-carbon tail was not involved in the reaction cascade but was accommodated by the larger active site cavity.

The near-complete CS-to-SS conversion is significant and is entirely consistent with the role of N338 in positioning a water as the α-terpinyl cation (**31**) capture nucleophile. The lack of reciprocity in the SS-to-CS conversion suggests that the active site structure of SS is quite different, and the role of this N in the SS mutant must be considered in the context of the surrounding cavity. The function of a similarly placed N in the olefinic cyclase (−)-LS is certainly also different from CS. The subtlety of active site structure–function relationships was demonstrated in directed mutagenesis studies performed on two sets of closely related conifer monoterpene cyclases that showed product outcome to require the collective interaction of multiple amino acid changes.[115,116] Clearly, the relationship between structure and function in the terpene cyclases is often difficult to assess; the reaction sequences are complex and defining the role of active site residues in the reaction cascades is rarely as straightforward as in the case of CS.

1.15.4 Conclusions

Notable progress has been made in the past decade in elucidating monoterpene cyclase reaction stereochemistry and mechanism. Molecular biology has greatly expanded the availability of, and access to, scores of terpene cyclases, including monoterpene cyclases that produce most structural types. Crystal structures have been determined for three catalytically unique monoterpene cyclases, and several important mechanistic features of these enzymes have been confirmed by this structural work. Progress made during the past decade is substantial and informative, and it is clear that structural analysis of cyclases bound with nonreactive analogs has been particularly fruitful when coupled with structure-guided site-directed mutagenesis. Acquiring structures of alternate cyclases of multiple types and of different stereochemistries is a priority for the future. When coupled with mechanistic, biochemical, and mutagenic studies of these enzymes, structural evaluation can provide enormous insight into monoterpene cyclization cascades of considerable complexity.

Acknowledgments

I would like to thank Professor Rodney Croteau for critical reading of this manuscript and for helpful comments. Financial support was provided by the NIH.

References

1. J. Gershenzon; N. Dudareva, *Nat. Chem. Biol.* **2007**, *3*, 408.
2. J. B. Harborne, Recent Advances in the Ecological Chemistry of Plant Terpenoids. In *Ecological Chemistry and Biochemistry of Plant Terpenoids*; J. B. Harborne, F. A. Tomas-Barberan, Eds.; Clarendon: Oxford, 1991; Vol. 31, p 399.
3. J. Gershenzon; R. Croteau, Terpenoids. In Herbivores: *Their Interaction with Secondary Metabolites*; G. A. Rosenthal, M. Berenbaum, Eds.; Academic Press: New York, 1991; p 165.
4. M. A. Phillips; R. Croteau, *Trend Plant Sci.* **1999**, *4*, 184.
5. R. Croteau; E. M. Davis; K. L. Ringer; M. R. Wildung, *Naturwissenschaften* **2005**, *92*, 562.
6. R. Croteau; C. L. Hooper, *Plant Physiol.* **1978**, *61*, 737.
7. R. Croteau; C. Martinkus, *Plant Physiol.* **1979**, *64*, 169.
8. R. Croteau, *Chem. Rev.* **1987**, *87*, 929.
9. M. L. Wise; R. Croteau, Monoterpene Biosynthesis. In *Comprehensive Natural Products Chemistry: Isoprenoids Including Steroids and Carotenoids*; D. E. Cane, Ed.; Elsevier Science: Oxford, 1999; Vol. 2, p 97.
10. E. M. Davis; R. Croteau, Cyclization Enzymes in the Biosynthesis of Monoterpenes, Sesquiterpenes and Diterpenes. In *Topics in Current Chemistry: Biosynthesis – Aromatic Polyketides, Isoprenoids, Alkaloids*; F. Leeper, J. C. Vederas, Eds.; Springer-Verlag: Heidelberg, Germany, 2000; Vol. 209, p 53.
11. D. B. Little; R. Croteau, Biochemistry of Essential Oil Terpenes. A Thirty Year Overview. In *Flavor Chemistry: Thirty Years of Progress*; I. Hornstein, E. L. Wick, R. Teranashi, Eds.; Kluwer Academic, Plenum Press: New York, 1999; p 239.
12. R. Croteau; T. M. Kutchan; N. G. Lewis, Natural Products (Secondary Metabolites). In *Biochemistry and Molecular Biology of Plants*; B. B. Buchanan, W. Gruissem, R. L. Jones, Eds.; American Society of Plant Physiologists: Rockville, MD, 2000; p 1250.
13. T. Koyama; K. Ogura, Isopentenyl Diphosphate Isomerase and Prenyltranferases. In *Comprehensive Natural Products Chemistry: Isoprenoids Including Steroids and Carotenoids*; D. E. Cane, Ed.; Elsevier Science: Oxford, 1999; Vol. 2, p 69.
14. C. D. Poulter; H. C. Rilling, Prenyl Transferases and Isomerase. In *Biosynthesis of Isoprenoid Compounds*; J. W. Porter, S. L. Spurgeon, Eds.; Wiley: New York, 1981; Vol. 1, p 162.
15. H. V. Thulasiram; H. K. Erickson; C. D. Poulter, *Science* **2007**, *316*, 73.
16. D. W. Christianson, *Chem. Rev.* **2006**, *106*, 3412.
17. R. Croteau; D. E. Cane, Monoterpene and Sesquiterpene Cyclases. In *Methods Enzymology*; J. H. Law, H. C. Rilling, eds.; Academic Press: New York, 1985; Vol. 110, p 383.
18. A. Saito; H. C. Rilling, *Arch. Biochem. Biophys.* **1981**, *208*, 508.
19. V. J. Davisson; T. R. Neal; C. D. Poulter, *J. Am. Chem. Soc.* **1985**, *107*, 5277.
20. A. B. Gilg; C. Tittiger; G. J. Blomquist, *Naturwissenschaften* **2009**, *96*, 731.
21. S. Green; E. N. Friel; A. Matich; L. L. Beuning; J. M. Cooney; D. D. Rowan; E. MacRae, *Phytochemistry* **2007**, *68*, 176.
22. D. E. Cane, Sesquiterpene Biosynthesis: Cyclization Mechanisms. In *Comprehensive Natural Products Chemistry: Isoprenoids Including Steroids and Carotenoids*; D. E. Cane, Ed.; Elsevier Science: Oxford, 1999; Vol. 2, p 155.
23. M. A. Phillips; M. R. Wildung; D. C. Williams; D. C. Hyatt; R. Croteau, *Arch. Biochem. Biophys.* **2003**, *411*, 267.
24. C. G. Jones; C. I. Keeling; E. L. Ghisalberti; E. L. Barbour; J. A. Plummer; J. Bohlmann, *Arch. Biochem. Biophys.* **2008**, *477*, 121.
25. R. Croteau; F. Karp, *Arch. Biochem. Biophys.* **1977**, *179*, 257.
26. R. Croteau; F. Karp, *Arch. Bioch. Biophys.* **1979**, *198*, 512.
27. R. Croteau; M. Felton; R. C. Ronald, *Arch. Bioch. Biophys.* **1980**, *200*, 534.
28. H. Gambliel; R. Croteau, *J. Biol. Chem.* **1982**, *257*, 2335.
29. R. Kjonaas; R. Croteau, *Arch. Bioch. Biophys.* **1983**, *220*, 79.
30. R. Croteau; F. Karp, *Arch. Bioch. Biophys.* **1979**, *198*, 523.
31. A. L. Schilmiller; I. Schauvinhold; M. Larson; R. Xu; A. L. Charbonneau; A. Schmidt; C. Wilkerson; R. L. Last; E. Pichersky, *Proc. Natl. Acad. Sci. U.S.A.* **2009**, *106*, 10865.
32. C. Sallaud; D. Rontein; S. Onillon; F. Jabès; P. Duffé; C. Giacalone; S. Thoraval; C. Escoffier; G. Herbette; M. Leonhardt; A. Causse; A. Tissier, *Plant Cell* **2009**, *21*, 301.
33. C. C. Burke; M. R. Wildung; R. Croteau, *Proc. Natl. Acad. Sci. U.S.A.* **1999**, *96*, 13062.
34. F. Bouvier; C. Suire; A. d'Harlingue; R. A. Backhaus; B. Camara, *Plant J.* **2000**, *24*, 241.
35. C. Burke; R. Croteau, *Arch. Biochem. Biophys.* **2002**, *405*, 130.
36. D. Tholl; C. M. Kish; I. Orlova; D. Sherman; J. Gershenzon; E. Pichersky; N. Dudareva, *Plant Cell* **2004**, *16*, 977.
37. Y.-Y. Hsiao; M.-F. Jeng; W.-C. Tsai; Y.-C. Chuang; C.-Y. Li; T.-S. Wu; C.-S. Kuoh; W.-H. Chen; H.-H. Chen, *Plant J.* **2008**, *55*, 719.
38. A. Schmidt; J. Gershenzon, *Phytochemistry* **2008**, *69*, 49.
39. G. Wang; R. A. Dixon, *Proc. Natl. Acad. Sci. U.S.A.* **2009**, *106*, 9914.
40. K. P. Adams; R. Croteau, *Phytochemistry* **1998**, *49*, 475.
41. K. P. Adams; J. E. Crock; R. Croteau, *Arch. Biochem. Biophys.* **1996**, *332*, 352.
42. M. Wise; G. L. Rorrer; J. J. Polzin; R. B. Croteau, *Arch. Biochem. Biophys.* **2002**, *400*, 125.
43. C.-M. Wang; D. E. Cane, *J. Am. Chem. Soc.* **2008**, *130*, 8908.
44. M. Komatsu; M. Tsuda; S. Omura; H. Oikawa; H. Ikeda, *Proc. Natl. Acad. Sci. U.S.A.* **2008**, *105*, 7422.
45. T. W. Hallahan; R. Croteau, *Arch. Biochem. Biophys.* **1988**, *264*, 618.
46. R. Croteau; N. M. Felton; C. J. Wheeler, *J. Biol. Chem.* **1985**, *260*, 5956.
47. D. M. Satterwhite; C. J. Wheeler; R. Croteau, *J. Biol. Chem.* **1985**, *260*, 13901.
48. T. W. Hallahan; R. Croteau, *Arch. Biochem. Biophys.* **1989**, *269*, 313.
49. T. J. Savage; R. Croteau, *Arch. Biochem. Biophys.* **1993**, *305*, 581.
50. G. Portilla; M. C. Rojas; L. Chayet; O. Cori, *Arch. Biochem. Biophys.* **1982**, *218*, 614.
51. L. Chayet; M. C. Rojas; E. Cardemil; A. M. Jabalquinto; R. Vicuña; O. Cori, *Arch. Biochem. Biophys.* **1977**, *180*, 318.
52. R. Croteau, *Arch. Biochem. Biophys.* **1986**, *251*, 777.
53. F. Karp; R. Croteau, *Arch. Biochem. Biophys.* **1994**, *309*, 184.

54. C. D. Poulter; J. C. Argyle; E. A. Mash, *J. Biol. Chem.* **1978**, *253*, 7227.
55. C. D. Poulter; D. M. Satterwhite, *Biochemistry* **1977**, *16*, 5470.
56. F. Karp; Y. Zhao; B. Santhamma; B. Assink; R. M. Coates; R. B. Croteau, *Arch. Biochem. Biophys.* **2007**, *468*, 140.
57. C. J. Wheeler; R. Croteau, *Arch. Biochem. Biophys.* **1986**, *246*, 733.
58. C. J. Wheeler; R. Croteau, *Proc. Natl. Acad. Sci. U.S.A.* **1987**, *84*, 4856.
59. W. Schwab; D. C. Williams; E. M. Davis; R. Croteau, R, *Arch. Biochem. Biophys.* **2001**, *392*, 123.
60. D. C. Hyatt; B. Youn; Y. Zhao; B. Santhamma; R. M. Coates; R. B. Croteau; C. H. Kang, *Proc. Natl. Acad. Sci. U.S.A.* **2007**, *104,* 5360.
61. R. Croteau; D. M. Satterwhite; D. E. Cane; C. C. Chang, *J. Biol. Chem.* **1986**, *261*, 13438.
62. R. Croteau; D. M. Satterwhite; C. J. Wheeler; N. M. Felton, *J. Biol. Chem.* **1989**, *264*, 2075.
63. R. Croteau; D. M. Satterwhite; D. E. Cane; C. C. Chang, *J. Biol. Chem.* **1988**, *263*, 10063.
64. S. Aubourg; A. Lecharny; J. Bohlmann, *Mol. Genet. Genomics* **2002**, *267*, 730.
65. G. A. Tuskan; S. Difazio; S. Jansson; J. Bohlmann; I. Grigoriev; U. Hellsten; N. Putnam; S. Ralph; S. Rombauts; A. Salamov; J. Schein; L. Sterck; A. Aerts; R. R. Bhalerao; R. P. Bhalerao; D. Blaudez; W. Boerjan; A. Brun; A. Brunner; V. Busov; M. Campbell; J. Carlson; M. Chalot; J. Chapman; G. L. Chen; D. Cooper; P. M. Coutinho; J. Couturier; S. Covert; Q. Cronk; R. Cunningham; J. Davis; S. Degroeve; A. Déjardin; C. Depamphilis; J. Detter; B. Dirks; I. Dubchak; S. Duplessis; J. Ehlting; B. Ellis; K. Gendler; D. Goodstein; M. Gribskov; J. Grimwood; A. Groover; L. Gunter; B. Hamberger; B. Heinze; Y. Helariutta; B. Henrissat; D. Holligan; R. Holt; W. Huang; N. Islam-Faridi; S. Jones; M. Jones-Rhoades; R. Jorgensen; C. Joshi; J. Kangasjärvi; J. Karlsson; C. Kelleher; R. Kirkpatrick; M. Kirst; A. Kohler; U. Kalluri; F. Larimer; J. Leebens-Mack; J. C. Leplé; P. Locascio; Y. Lou; S. Lucas; F. Martin; B. Montanini; C. Napoli; D. R. Nelson; C. Nelson; K. Nieminen; O. Nilsson; V. Pereda; G. Peter; R. Philippe; G. Pilate; A. Poliakov; J. Razumovskaya; P. Richardson; C. Rinaldi; K. Ritland; P. Rouzé; D. Ryaboy; J. Schmutz; J. Schrader; B. Segerman; H. Shin; A. Siddiqui; F. Sterky; A. Terry; C. J. Tsai; E. Uberbacher; P. Unneberg; J. Vahala; K. Wall; S. Wessler; G. Yang; T. Yin; C. Douglas; M. Marra; G. Sandberg; Y. Van de Peer; D. Rokhsar, *Science* **2006**, *313*, 1596.
66. O. Jaillon; J. M. Aury; B. Noel; A. Policriti; C. Clepet; A. Casagrande; N. Choisne; S. Aubourg; N. Vitulo; C. Jubin; A. Vezzi; F. Legeai; P. Hugueney; C. Dasilva; D. Horner; E. Mica; D. Jublot; J. Poulain; C. Bruyère; A. Billault; B. Segurens; M. Gouyvenoux; E. Ugarte; F. Cattonaro; V. Anthouard; V. Vico; C. Del Fabbro; M. Alaux; G. Di Gaspero; V. Dumas; N. Felice; S. Paillard; I. Juman; M. Moroldo; S. Scalabrin; A. Canaguier; I. Le Clainche; G. Malacrida; E. Durand; G. Pesole; V. Laucou; P. Chatelet; D. Merdinoglu; M. Delledonne; M. Pezzotti; A. Lecharny; C. Scarpelli; F. Artiguenave; M. E. Pè; G. Valle; M. Morgante; M. Caboche; A. F. Adam-Blondon; J. Weissenbach; F. Quétier; P. Wincker; *Nature* **2007**, *449*, 463.
67. J. Bohlmann; G. Meyer-Gauen; R. Croteau, *Proc. Natl. Acad. Sci. U.S.A.* **1998**, *95*, 4126.
68. S. Aubourg; A. Lecharny; J. Bohlmann, *Mol. Genet. Genomics* **2002**, *267*, 730.
69. D. M. Martin; J. Fäldt; J. Bohlmann, *Plant Physiol.* **2004**, *135*, 1908.
70. S. C. Trapp; R. B. Croteau, *Genetics* **2001**, *158*, 811.
71. B. S. Lee; J. Chappell, *Plant Physiol.* **2008**, *147*, 1017.
72. K. U. Wendt; G. E. Schulz, *Structure* **1998**, *6*, 127.
73. D. A. Whittington; M. L. Wise; M. Urbansky; R. M. Coates; R. B. Croteau; D. W. Christianson, *Proc. Natl. Acad. Sci. U.S.A.* **2002**, *99*, 15375.
74. L. C. Tarshis; M. Lan; C. D. Poulter; J. C. Sacchettini, *Biochemistry* **1994**, *33*, 10871.
75. C. A. Lesburg; G. Zhai; D. E. Cane; D. W. Christianson, *Science* **1997**, *277*, 1820.
76. R. J. Peters; M. M. Ravn; R. M. Coates; R. B. Croteau, *J. Amer. Chem. Soc.* **2001**, *123*, 8974.
77. C. M. Starks; K. Back; J. Chappell; J. P. Noel, *Science* **1997**, *277*, 1815.
78. S. C. Kampranis; D. Ioannidis; A. Purvis; W. Mahrez; E. Ninga; N. A. Katerelos; S. Anssour; J. M. Dunwell; J. Degenhardt; A. M. Makris; P. W. Goodenough; C. B. Johnson, *Plant Cell* **2007**, *19*, 1994.
79. M. K. El Tamer; J. Lücker; D. Bosch; H. A. Verhoeven; F. W. A. Verstappen; W. Schwab; A. J. van Tunen; A. G. J. Voragen; R. A. de Maagd; H. J. Bouwmeester, *Arch. Biochem. Biophys.* **2003**, *411*, 196.
80. R. J. Peters; R. B. Croteau, *Arch. Biochem. Biophys.* **2003**, *417*, 203.
81. K. Back; J. Chappell, *Proc. Natl. Acad. Sci. U.S.A.* **1996**, *93*, 6841.
82. E. Y. Shishova; F. Yu; D. J. Miller; J. A. Faraldos; Y. Zhao; R. M. Coates; R. K. Allemann; D. E. Cane; D. W. Christianson, *J. Biol. Chem.* **2008**, *283*, 15431.
83. J. Bohlmann; M. Phillips; V. Ramachandiran; S. Katoh; R. Croteau, *Arch. Biochem. Biophys.* **1999**, *368*, 232.
84. D. M. Martin; J. Fäldt; J. Bohlmann, *Plant Physiol.* **2004**, *136*, 3724.
85. J. Bohlmann; C. L. Steele; R. Croteau, *J. Biol. Chem.* **1997**, *272*, 21784.
86. J. Fäldt; D. M. Martin; B. Miller; S. Rawat; J. Bohlmann, *Plant Mol. Biol. Rep.* **2003**, *51*, 119.
87. J. Lucker; M. K. El Tamer; W. Schwab; F. W. A. Verstappen; L. H. W. van der Plas; H. J. Bouwmeester; H. A. Verhoeven, *Eur. J. Biochem.* **2002**, *269*, 3160.
88. D. M. Martin; J. Bohlmann, *Phytochemistry* **2004**, *65*, 1223.
89. M. L. Wise; T. J. Savage; E. Katahira; R. Croteau, *J. Biol. Chem.* **1998**, *273*, 14891.
90. Y. Iijima; R. Davidovich-Rikanati; E. Fridman; D. R. Gang; E. Bar; E. Lewinsohn; E. Pichersky, *Plant Physiol.* **2004**, *136*, 3724.
91. S. M. Colby; W. R. Alonso; E. J. Katahira; D. J. McGarvey; R. Croteau, *J. Biol. Chem.* **1993**, *268*, 23016.
92. S. Green; C. J. Squire; N. J. Nieuwenhuizen; E. N. Baker; W. Laing, *J. Biol. Chem.* **2009**, *284*, 8661.
93. T. Suga; Y. Hiraga; W. A. Mie; S. Isumi, *J. Chem. Soc. Chem. Commun.* **1992**, 1556.
94. Y. Hiraga; W. Shi; D. I. Ito; S. Ohta; T. Suga, *J. Chem. Soc. Chem. Commun.* **1993**, 1370.
95. H.-J. Pyun; R. M. Coates; K. C. Wagschal; P. McGeady; R. B. Croteau, *J. Biol. Chem.* **1993**, *58*, 3998.
96. M. F. Leopold; W. W. Epstein; D. M. Grant, *J. Am. Chem. Soc.* **1988**, *110*, 616.
97. J. I. M. Rajaonarivony; J. Gershenzon; R. Croteau, *Arch. Biochem. Biophys.* **1992**, *296*, 49.
98. W. R. Alonso; J. I. M. Rajaonarivony; J. Gershenzon; R. Croteau, *J. Biol. Chem.* **1992**, *267*, 7582.
99. G. Turner; J. Gershenzon; E. E. Nielson; J. E. Froehlich; R. Croteau, *Plant Physiol.* **1999**, *120*, 879.
100. D. C. Williams; D. J. McGarvey; E. J. Katahira; R. Croteau, *Biochemistry* **1998**, *37*, 12213.

101. J. I. M. Rajaonarivony; J. Gershenzon; J. Miyazaki; R. Croteau, *Arch. Biochem. Biophys.* **1992**, *299*, 77.
102. R. Croteau; J. J. Shaskus; B. Renstrom; N. M. Felton; D. E. Cane; A. Saito; C. Chang, *Biochemistry* **1985**, *24*, 7077.
103. D. E. Cane; A. Saito; R. Croteau; J. Shaskus; N. M. Felton, *J. Am. Chem. Soc.* **1982**, *104*, 5831.
104. K. C. Wagschal; H.-J. Pyun; R. M. Coates; R. Croteau, *Arch. Biochem. Biophys.* **1994**, *308*, 477.
105. R. Croteau; C. J. Wheeler; D. E. Cane; R. Ebert; H.-J. Ha, *Biochemistry* **1987**, *26*, 5383.
106. M. L. Wise; H.-J. Pyun; G. Helms; B. Assink; R. M. Coates; R. B. Croteau, *Tetrahedron* **2001**, *57*, 5327.
107. R. Croteau; D. M. Satterwhite, *J. Biol. Chem.* **1989**, *264*, 15309.
108. F. Chen; D.-K. Ro; J. Petri; J. Gershenzon; J. Bohlmann; E. Pichersky; D. Tholl, *Plant Physiol.* **2004**, *135*, 1956.
109. J. G. Romagni; S. N. Allen; F. E. Dayan, *J. Chem. Ecol.* **2000**, *26*, 303.
110. J. P. Halligan, *Ecology* **1975**, *56*, 999.
111. I. R. Lawler; J. Stapley; W. J. Foley; B. M. Eschler, *J. Chem. Ecol.* **1999**, *25*, 401.
112. R. Croteau; W. R. Alonso; A. E. Koepp; M. A. Johnson, *Arch. Biochem. Biophys.* **1994**, *309*, 184.
113. M. L. Wise; M. Urbansky; G. L. Helms; R. M. Coates; R. Croteau, *J. Am. Chem. Soc.* **2002**, *124*, 8546.
114. T. G. Kolner; C. Schnee; J. Gershenzon; J. Degenhardt, *Plant Cell* **2004**, *16*, 1115.
115. D. C. Hyatt; R. Croteau, *Arch. Biochem. Biophys.* **2005**, *439*, 222.
116. S. Katoh; D. Hyatt; R. Croteau, *Arch. Biochem. Biophys.* **2004**, *425*, 65.

Biographical Sketch

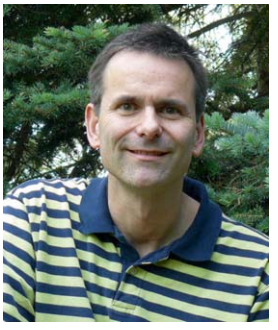

Edward M. Davis was born in Buffalo, NY, but spent his youth in Michigan City, IN. He is currently an assistant scientist in the laboratory of Professor Rodney Croteau (Institute of Biological Chemistry, Washington State University) working on monoterpene biosynthesis in mint and the structure–function relationship in monoterpene cyclases. He earned his B.S. in 1987 (Biological Sciences) and his Ph.D. in 1999 (Biochemistry and Molecular Biology) from Oklahoma State University in Stillwater, OK. He did his doctoral work with Dr. Margaret Essenberg where he studied a sesquiterpene cyclase that catalyzes the first committed step in phytoalexin production in *Gossypium hirsutum* (cotton).